A quantitative view on multivalent nanomedicine targeting

Advanced Drug Delivery Reviews 169 (2021) 1–21

Contents lists available at ScienceDirect

Advanced Drug Delivery Reviews

journal homepage: www.elsevier.com/locate/addr

A quantitative view on multivalent nanomedicine targeting

Laura Woythe [a], Nicholas B. Tito [b], Lorenzo Albertazzi [a,c,*]

[a] Department of Biomedical Engineering, Institute of Complex Molecular Systems (ICMS), Eindhoven University of Technology (TUE), Eindhoven 5612 AZ, the Netherlands
[b] Electric Ant Lab, Science Park 106, 1098 XG Amsterdam, the Netherlands
[c] Institute for Bioengineering of Catalonia (IBEC), The Barcelona Institute of Science and Technology (BIST), Barcelona 08036, Spain

ARTICLE INFO

Article history:
Received 14 May 2020
Received in revised form 11 November 2020
Accepted 21 November 2020
Available online 29 November 2020

Key words:
Nanotechnology
Rational design
Multivalency
Super-selectivity
Quantitative characterization

ABSTRACT

Although the concept of selective delivery has been postulated over 100 years ago, no targeted nanomedicine has been clinically approved so far. Nanoparticles modified with targeting ligands to promote the selective delivery of therapeutics towards a specific cell population have been extensively reported. However, the rational design of selective particles is still challenging. One of the main reasons for this is the lack of quantitative theoretical and experimental understanding of the interactions involved in cell targeting. In this review, we discuss new theoretical models and experimental methods that provide a quantitative view of targeting. We show the new advancements in multivalency theory enabling the rational design of super-selective nanoparticles. Furthermore, we present the innovative approaches to obtain key targeting parameters at the single-cell and single molecule level and their role in the design of targeting nanoparticles. We believe that the combination of new theoretical multivalent design and experimental methods to quantify receptors and ligands aids in the rational design and clinical translation of targeted nanomedicines.

Contents

Abbreviations: Bicinchonic acid, (BCA); DNA points accumulation for imaging in nanoscale topography, (DNA-PAINT); Epidermal growth factor receptor, (EGFR); Enzyme-linked immunosorbent assay, (ELISA); Fragment antigen-binding, (Fab); Fluorescence-activated cell sorting, (FACS); Fragment crystallizable region, (Fc); Quartz crystal microbalance, (QCM); Human epidermal growth factor receptor 2, (HER2); High-performance liquid chromatography, (HPLC); Immunohistochemistry, (IHC); Single-molecule localization microscopy, (SMLM); Surface plasmon resonance, (SPR); Stimulated emission depletion, (STED); stochastic optical reconstruction microscopy, (STORM); Transmission electron microscopy, (TEM)..

* Corresponding author at: Department of Biomedical Engineering, Institute of Complex Molecular Systems (ICMS), Eindhoven University of Technology (TUE), Eindhoven 5612 AZ, the Netherlands

E-mail addresses: l.woythe@tue.nl (L. Woythe), nicholas.b.tito@gmail.com (N.B. Tito), L.Albertazzi@tue.nl (L. Albertazzi).

https://doi.org/10.1016/j.addr.2020.11.010

1. Introduction: the challenges of active targeted nanomedicines

Nanomedicine employs nanotechnology to design drug delivery systems to engineer or cure the tissue of interest. Thirty years ago, the use of nanocarriers such as nanoparticles to selectively deliver therapeutic agents opened a spectrum of new opportunities: administer water-insoluble drugs, increase the drug accumulation in the tissue of interest and reduce the side effects of current therapeutics [1,2]. These advantages boosted the number of publications in the field and culminated in the first clinically approved nanomedicine in the mid-90s [3]. The benefits of nanomedicines were recognized in a variety of fields, including oncology, cardiology, vaccinology, and tissue engineering [4–8].

Off-target effects result in unwanted toxicities to healthy cells and are a significant bottleneck in the development of new therapies. Active targeting has been proposed to be the holy grail of nanomedicine, ensuring tissue and cell specificity [9]. In this approach, the nanocarrier is functionalized with targeting ligands– including antibodies, peptides, aptamers or other small molecules – able to bind selectively to a cell surface biomarker, guiding the nanoparticles to a specific organ or cell type [10]. Cells express a multitude of different biomarkers or receptors on their surface, which serve as hubs of chemical correspondence with other cells or biomolecules [11–22]. The expression level of these receptors generally changes, e.g. with overexpression in response to a tissue pathology or injury. This distinctive feature provides a possibility to selectively recognize only the diseased cells, opening an opportunity for nanomedicine targeting [23]. For example, some cancers highly express the human epidermal growth factor receptors 1 (EGFR) and 2 (HER2) [24], vascular cell adhesion molecule-1 is upregulated in kidney ischemia-reperfusion injury [25] and angiotensin II type I receptor is overexpressed in the myocardium during a heart attack [26]. Therefore, the successful design of actively targeted therapies would translate into a variety of clinical applications.

One of the main advantages of nanoparticles is the possibility of multivalent targeting via multiple ligand moieties [27]. In general terms, microscopic objects that interact with each other via multiple independent ligand-receptor bonds are called *multivalent* [11,12,28–33]. Multivalent binding is a uniquely selective interaction, compared to monovalent binding, due to both enthalpy and ligand/receptor combinatorial entropy playing a pivotal role in the binding thermodynamics. In nature, multivalent interactions promote the success of viruses and bacteria to infect their host cells [13,34–39]. These examples inspired the synthesis of synthetic multivalent constructs [31,32,40–52], including multivalent nanoparticles. Most engineered active-targeted nanoparticles can have more than one copy of the targeting ligand, which facilitates multiple binding of receptor-ligand pairs [53,54].

Despite the great promise and intense activity in this field during the last decades, active targeting of nanoparticles has been disappointing in the clinic, with no approved therapy so far [55]. Possible reasons for their poor clinical translation include the low accumulation of nanoparticles at the site of action, the lack of translation from mouse models to humans and the absent pre-selection of patients that could benefit from nanomedicine therapy [56,57]. The above is currently causing an increasing concern regarding the added value of actively targeted nanomedicines over their non-targeted counterparts [58,59]. A better understanding of the hurdles and pitfalls of active targeting is required to overcome these limitations [23,60].

Although active targeting is already implemented in clinical applications such as antibody-drug conjugates [61,62], the conjugation of targeting ligands to nanoparticles is more complex. Nanoparticles are bigger, have distinct physicochemical properties depending on their material, and the number and accessibility of conjugated targeting ligands on their surface are poorly understood. The added complexity of targeted nanoparticles triggers the question: is our picture of targeting too simplistic, and does this hamper the design of successful nanomedicines? We aim to address this question in the next paragraphs by briefly outlining the possible bottlenecks that slow down their clinical translation.

The first issue to consider is that nanoparticles must overcome numerous biological barriers inside the body before interacting with the target receptor [63–65]. Intravenously injected nanoparticles are prone to interact with serum proteins upon contact with the biological environment in the blood vessels, referred to as protein corona formation [66–68]. The protein corona formation can influence the physicochemical properties of nanoparticles affecting their stability or targeting ability [69]. In the latter case, protein corona formation can shield targeted nanoparticles and promote their uptake and elimination by specialized phagocytic cells (such as macrophages) reducing their efficiency to bind to receptors at the target site [70–72]. Nanoparticles must extravasate to the tissue of interest to reach their target, overcoming biological barriers such as the endothelial cells that compose the blood vessels walls [64,73] or the blood-brain-barrier [74,75]. Moreover, the dense mesh of fibers and cell networks that compose the extracellular matrix limits their diffusion [76,77]. Altogether, these factors might prevent targeting even before a nanoparticle can reach the desired cell. A detailed discussion of these biological barriers is beyond the purpose of this review but extensively explored elsewhere [63,64,78,79].

Once nanoparticles overcome these barriers, the cellular targeting can take place. Active-targeted nanoparticles have often been perceived as 'magic bullets' that are perfectly monodisperse and target the diseased cells exclusively as shown schematically in Fig. 1. For this ideal concept to be accurate, diseased cells would have to express a unique receptor that is absent in healthy cells (Fig. 1A). Recent advances in the field are starting to uncover the real picture behind active targeting (Fig. 1B), that is far from the idealistic concept of magic bullets. At the cellular level, we now know that common targets are not solely expressed in the diseased cells but also in the healthy ones. For example, epidermal growth factor and transferrin receptors are also expressed in the skin and liver besides being overexpressed in some cancers [80]. Thus, off-target effects are likely to happen. Additionally, the receptor expression between patients is highly heterogeneous, which translates into different therapeutic efficiencies amongst them [81–83].

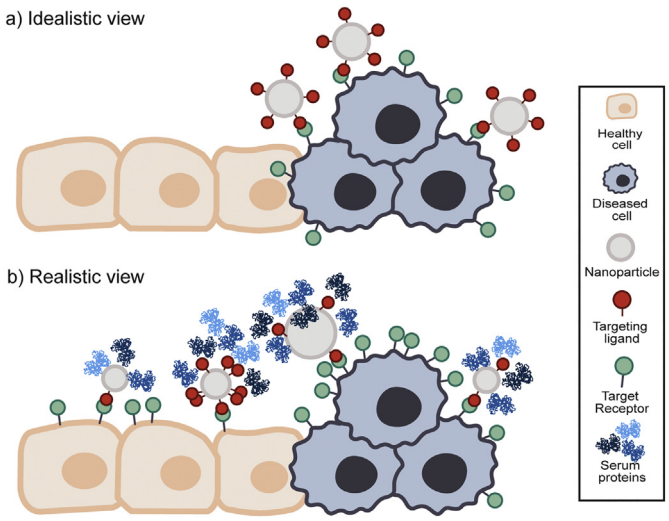

Fig. 1. Idealistic *versus* realistic view of active targeting nanomedicines (not to scale). In (A) an idealistic view of targeting is represented. The target cell receptor is exclusively expressed in the diseased cells and the homogeneous nanoparticle formulation interacts exclusively with targets on the diseased cells. (B) represents a more realistic view of targeting. The target cell receptor is expressed in the diseased and partially in healthy cells, leading to off-targeting. The receptor expression in the diseased cells is highly heterogeneous. Nanoparticles are heterogeneous in size and number of targeting ligands. These ligands can be shielded by overcrowding or serum proteins forming a protein corona, influencing the target recognition of the nanoformulation. Serum proteins are schematically represented by transferrin molecules (PDB ID 1D3K) [92].

At the nanoparticle level, reports are starting to uncover the heterogeneity in size, charge, and number of targeting ligands [84–86]. In fact, not all particles are conjugated with the same number of ligands but follow a broad distribution [87]. This distribution causes a significant difference in how individual nanoparticles interact with the target and the biological environment [88]. There is also a strong indication that ligands can lose their functionality upon conjugation due to denaturation, unfavourable orientation or shielding of binding sites due to overcrowding or protein corona formation [69,89]. Many nanomedicine designs overlook these challenges and underestimate the innate heterogeneity and complexity of these formulations, thereby minimizing the chances of successful targeting and treatment [90,91].

The rational design of nanoparticles requires accurate knowledge of both cell receptor expression and nanoparticle ligand number. Additionally, theoretical models of multivalent nanoparticle interactions have shown that these parameters are essential to achieve a higher selectivity towards a cell population of interest. However, quantifying the number of cell receptors and targeting ligands on nanoparticles is far from being trivial. Standard characterization techniques to quantify the receptor expression are semi-quantitative at best, and ligand-coated nanoparticles are often poorly characterized [93]. Because of the small size of receptor molecules and targeting ligands, quantitative characterization tools at a molecular level are highly desired [94,95].

In this review, we aim to address the state-of-the-art quantitative tools to understand, predict and design selective nanomedicine targeting towards cells or tissues of interest. Based on the established concept of multivalent binding, recent advances in theoretical modelling opened the door towards the design of super-selective nanomedicines, that will be discussed more extensively in the following section. In parallel, new quantitative experimental characterization techniques arose in recent years [96]. Single-cell and molecule approaches are necessary for guiding the design of targeted nanomedicines, providing crucial molecular information of both cell receptors and nanoparticle targeting ligands. For this reason, methods that provide numbers or distributions of receptors and ligands will be the main focus of this review. In particular, the development of new imaging tools such as super-resolution optical microscopy enabled molecular resolution of both cell and nanoparticle features. We believe that the combination of theoretical modelling and experimental methodologies will provide a better molecular picture of targeting that allows for the rational design of successful nanomedicines.

2. Towards understanding targeting at a molecular level

In this section, we will focus on quantitative theoretical and experimental tools that aid in the rational design of multivalent nanomedicines. First, we will review the advances in the prediction of the selectivity of multivalent nanoparticles in terms of simple thermodynamics. We will explore how multivalent interactions between targets and ligands can be tuned to enhance binding selectivity and translate the theoretical knowledge into guidelines for the rational design of super-selective nanomedicines. To effectively make use of such theory, quantitative methods to characterize nanomedicine targeting at a molecular level will be necessary. To this aim, we will first focus on the methods to characterize cell receptors. Next, methods to characterize nanoparticle targeting ligands will be reviewed. Special attention will be dedicated to the emerging single-cell and single-particle methods that allow a quantitative understanding of targeting at the molecular level.

2.1. The multivalent effect: theory and utilization of super-selectivity

2.1.1. A brief introduction to the thermodynamics of multivalent binding

Multivalency has become recognized as one of the central principles of targeting. As a result, extensive theoretical and computational work has been done to examine multivalent binding in model scenarios. In this section, we briefly outline the core principles of multivalency from the perspective of statistical thermodynamics. To showcase the theoretical principles simply and clearly, we focus on “homovalent” binding, where all ligands have the same chemistry on the multivalent particle. Heterovalent binding is touched upon in more descriptive terms in Section 2.1.3, while discussing applications of multivalent design.

Our discussion draws from theoretical results in Refs. [19,30,97]; we direct the reader to these papers for a more detailed exposition of multivalent binding thermodynamics for homo- and hetero-valent binding. These models have primarily focused on the multivalent binding itself, neglecting factors such as competition (e.g. from other biological or synthetic binders/ligands nearby), details on the steric accessibility of receptors for ligand binding, and kinetic barriers to binding (e.g. due to crowding by other entities near the cell membrane or local conformational/structural barriers). Following a few examples, we describe some of the ways to employ multivalent design in practice, and also highlight recent progress towards modelling multivalent binding in more realistic scenarios which incorporate some of the challenges above.

The binding free energy between two multivalent entities (e.g. nanoparticle and cell) contains both enthalpic and entropic contributions [30,31]. The enthalpic contribution to multivalent binding originates intuitively from the bonding between the ligands and receptors. A larger number of potential ligand-receptor bonds per multivalent particle means that it will have a larger, more negative, and more favorable enthalpic contribution to its binding free energy. In comparison,the entropic contribution is more subtle. Firstly, ligands and receptors lose configurational entropy whenever they form a bond. When bound, the ligand and receptor may only adopt molecular conformations that keep their binding groups attached to each other. There are fewer molecular conformations that satisfy this constraint, compared to when the two are not bound. This entropic penalty causes the “effective” ligand/receptor bond strength to be lower than what is observed between the two structures when they are free in solution [31,33].

On the other hand, an entropic *gain* comes from the fact that ligands and receptors may explore different binding combinations – more formally called “permutations”. For example, when the ligands and receptors are short and spaced far apart, then each ligand or receptor may be independently bound or unbound to its nearest partner. Thermal fluctuations drive each of these entities to attempt binding or unbinding over time. When the ligands and receptors are, in the other extreme, long and flexible, then each may be bound or unbound to multiple partners. A convenient visual example is to imagine that the ligands are like wires on a telephone switchboard, and the plugs are the receptors [52].

The permutation entropy grows larger and more favourable when there are more ligands and receptors on the two multivalent structures. Accordingly, the binding free energy ΔG_{bind} becomes more negative, and the binding probability grows exponentially larger (since this depends on $\exp(-\Delta G_{\mathrm{bind}}/RT)$).

The rapid growth in the binding probability as a function of the number of ligands and receptors on the two multivalent objects is called *super-selectivity*. In the super-selective regime, the logarithm of the number of surface-bound particles increases more sharply than linearly with the logarithm of the surface receptor concentration [30]. This means that a multivalent particle can be very specific for a certain density of receptors above a sharp threshold and therefore can be more selective for the diseased cells.

Super-selectivity is fundamentally an entropic effect, arising from the permutation entropy described above. For example, monovalent binders – those having only one single ligand – can never exhibit super-selective binding, since they lack the entropic permutation contribution to their binding free energy. Their bonding strength may only be modulated by the enthalpy of their (single) bond, which leads to standard Langmuir adsorption.

We now take a moment to illustrate how these thermodynamic contributions enter into the overall binding free energy of a multivalent particle, leading to some of the trends in selectivity noted here. The ensuing discussion draws on the core theoretical elements of multivalent binding derived in Refs. [19,30,97].

For demonstration, we consider the simple example of a solution of multivalent particles at a low molar concentration [C], each having N_L ligands, in contact with a large surface of mobile receptors at surface density σ_R (number of receptors per unit area). Each ligand-receptor bond contributes a binding free energy of ΔG_{lig}. This bond free energy includes the standard equilibrium constant K_i, as well as the extra entropic free energy cost $\Delta G_{\mathrm{lig,cnf}}$ for forming the ligand-receptor bond:

$$\frac{\Delta G_{\mathrm{lig}}}{RT} = -\ln\left(\frac{K_i}{N_{\mathrm{av}} v_{\mathrm{free}}}\right) + \frac{\Delta G_{\mathrm{lig,cnf}}}{RT} \qquad \text{(Eq.1)}$$

Here, N_{av} is Avogadro's number, and v_{free} is the microscopically-sized volume of space that the binding endpoints on the ligand and receptor may conformationally explore (relative to their respective points of attachment on their host) when they are not bound to each other. We return to suggestions for which value to choose for this microscopic variable shortly.

By Eq. 1, we see that for ligand designs that all have the same configurational free energy cost $\Delta G_{\mathrm{lig,cnf}}$ for bonding, ratios of the free solution ligand-receptor equilibrium constants K_i corresponds to additive differences in their receptor bonding free energy. This is a powerful link to experiment.

In the simple model scenario we have outlined here, the total binding free energy of the multivalent particles is given by

$$\frac{\Delta G_{\mathrm{bind}}}{RT} = -\widetilde{N}_{\mathrm{L}} \ln\left(1 + \widetilde{N}_{\mathrm{R}} e^{-\Delta G_{\mathrm{lig}}/\mathrm{RT}}\right) + \frac{\Delta G_{NS}}{RT} - \ln\left(N_{\mathrm{av}} v_{\mathrm{ex}}[\mathrm{C}]\right) \qquad \text{(Eq.2)}$$

The variables in this equation are shown schematically in Fig. 2A. The first term of this equation is the multivalent binding contribution. The quantity $\widetilde{N_R}$ is the number of receptors that are accessible to the particle when it is adjacent to the surface. This may be approximated by $\widetilde{N_R} = \sigma_R a^2$, where a is the diameter of a multivalent particle. The quantity a^2 is therefore the size of the "footprint" that one bound multivalent particle has on the receptor surface. Similarly, $\widetilde{N_L}$ is the number of ligands on a multivalent particle that are simultaneously in contact with the surface. When a multivalent particle is adjacent to the receptor surface, it can also have one or more additional "non-specific" (i.e. non-multivalent) interaction free energy contributions. These include interactions between inert parts of the ligands and receptors, between ligands and the cell membrane (or other constructs thereupon), or between the multivalent particle core and the cell membrane. Ionic charges may play a role in some of these interactions. All of these interactions are placed into the quantity ΔG_{NS}, shown as the second term in Eq.2. Finally, the third term represents the chemical potential of the multivalent particles in solution. In the schematic model above we have assumed ideal solution conditions, where the chemical potential depends logarithmically on the particle molar solution concentration [C], and the volume v_{ex} of a single particle.

The enthalpic contribution to the binding free energy in the first term of Eq.2 comes from the per-ligand bond strength ΔG_{lig}. The entropic contribution comes from the fact that each of the $\widetilde{N_L}$ ligands on a multivalent particle may be bound to any one of the $\widetilde{N_R}$ receptors in the particle's surface footprint. These two contributions can be seen most clearly by considering the limit where the ligands are very strong binding (large negative ΔG_{lig}), such that they are all bound to a receptor. In this case, Eq.2 reduces to

$$\frac{\Delta G_{\mathrm{bind}}}{RT} \approx \left[\frac{\widetilde{N_L}\Delta G_{\mathrm{lig}}}{\mathrm{RT}} - \widetilde{N}_{\mathrm{L}} \ln\left(\widetilde{N_R}\right)\right] + \frac{\Delta G_{NS}}{RT} - \ln\left(N_{av} v_{\mathrm{ex}}[\mathrm{C}]\right) \qquad \text{(Eq.3)}$$

The multivalent contribution is shown here in square brackets. The first term is the enthalpic part, containing the $\widetilde{N_L}$ ligand-receptor bonds each with bond strength ΔG_{lig}. The second term is the entropic contribution, coming from the permutations of $\widetilde{N_L}$ ligands with any of the $\widetilde{N_R}$ within the surface footprint of the multivalent particle.

One of the more ambiguous parameters in Eqs. 2-3 (through Eq. 1) is "v_{free}" – the volume of space that an unbound ligand and receptor may conformationally explore, relative to the points of attachment on their hosts. The choice of this quantity depends on the geometry of the overall multivalent interaction. For example, consider a multivalent particle with flexible ligands, interacting with a surface with very small ("point-like") mobile receptors. In this case, a single ligand may (approximately) explore the volume $v_{\mathrm{free}} = ha^2$, where h is the average width between the receptor surface and the surface of the multivalent particle when bound. (An unbound receptor has no such conformational freedom to account for in this example, as it is a point entity.) In this case, then Eq.2 simplifies to

$$\frac{\Delta G_{\mathrm{bind}}}{RT} = -\widetilde{N}_{\mathrm{L}} \ln\left(1 + \frac{\sigma_R K_i}{N_{av} h} e^{-\Delta G_{\mathrm{lig,cnf}}/\mathrm{RT}}\right) + \frac{\Delta G_{NS}}{RT} - \ln\left(N_{\mathrm{av}} v_{\mathrm{ex}}[\mathrm{C}]\right) \qquad \text{(Eq.4)}$$

This form of Eq. 2 showcases the concept of "effective molarity" of receptors [97], here represented by the factor (σ_R / N_{av} h). The effective receptor molarity is the concentration of surface receptors "seen" by a ligand on a bound multivalent particle. For other kinds of multivalent

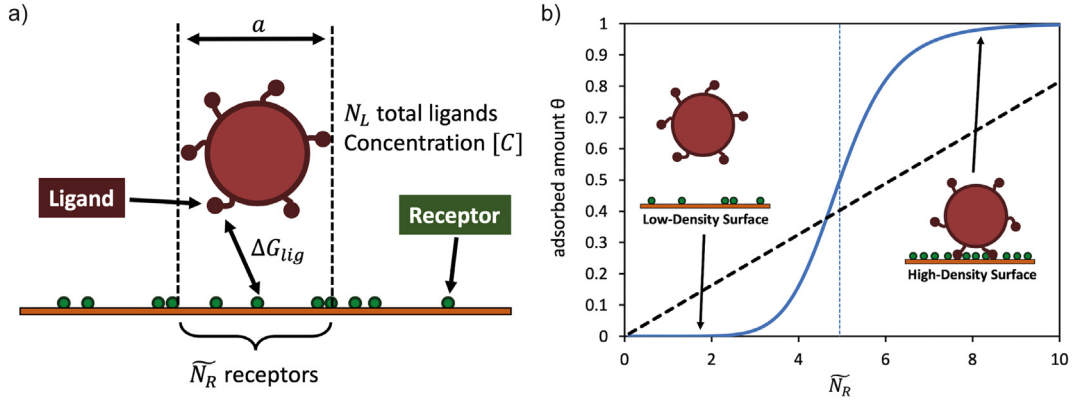

Fig. 2. (a) Schematic of a multivalent particle interacting with a receptor-coated surface. Symbols refer to the variables in Eq. 2. (b) Example of a multivalent binding adsorption curve (blue continuous line), with schematics of binding on surfaces with low and high receptor density. The binding transition is represented by the blue dashed line. Adsorption curve for receptor-sized monovalent binders is shown by the black dashed line for comparison.

binding constructs, v_{free} may be adapted based on the particular conformational flexibility of the ligands and receptors relative to their attachment points.

To finish, we link the binding free energy of a multivalent particle and the fraction "θ" of the target surface occupied by bound particles. This is calculated via the standard Langmuir adsorption isotherm,

$$\theta = \frac{e^{-\Delta G_{bind}/RT}}{1 + e^{-\Delta G_{bind}/RT}} \quad \text{(Eq.5)}$$

An example of a multivalent adsorption curve is shown in Fig. 2B, along with a comparable monovalent adsorption curve. As $\Delta G_{bind}/RT$ grows larger than zero – an unfavourable binding free energy – then θ goes to zero. On the other end, when $\Delta G_{bind}/RT$ grows larger and more negative, θ approaches 1. Thus, the choice of receptor density σ_R (via $\widetilde{N_R}$) where $\Delta G_{bind}/RT = 0$ corresponds to the binding transition. A sharper transition is more selective, in that the adsorption profile more closely resembles a step-like "all or nothing" form. On the other hand, Fig. 2B shows how monovalent binders respond only linearly to the density of receptors on the target surface regardless of whether they are weak- or strong-binding; they therefore exhibit no selective binding behaviour.

This discussion has entirely focused on the *equilibrium* thermodynamics of multivalent binding. However, the timescale it takes for a synthetic or natural multivalent system to reach equilibrium depends on the ligand-receptor binding kinetics, particularly when the ligands have long bond lifetimes – for example, due to large bond enthalpy or steep activation barriers to binding/unbinding [18,98–104]. Systems with large kinetic barriers exhibit long-lived intermediate states; these states are potentially more important to the application at hand than the equilibrium state itself, depending on the timescale of the application.

2.1.2. Influence of multivalent design parameters on targeting selectivity

Equation 2 is an example of how multivalent binding strength generally depends on:

- the multivalent particle design, through the number of ligands N_L per particle;
- the surface receptor density σ_R;
- ligand and receptor chemical design, which defines the ligand-receptor bond strength ΔG_{lig};
- concentration [C] of multivalent particles in solution above the surface.
- additional non-specific interactions, contained in $\Delta G_{NS}/RT$, between multivalent particles and the cell membrane.

Fig. 3 shows examples of multivalent adsorption curves θ, as a function of the surface receptor density $\widetilde{N_R}$, in order to illustrate how these parameters influence the shape and shift of the adsorption profile.

The concentration [C] of the multivalent particles in solution shifts the binding free energy ΔG_{bind} in Eq.2 up or down by a constant. This parameter is therefore convenient for shifting the critical surface receptor density σ_R at which the adsorption transition occurs. Fig. 3A shows a few examples. A smaller concentration [C] leads to a more unfavourable (larger and more positive) free energy of binding. This causes the inflection point of the adsorption profile to shift to larger receptor density σ_R.

The non-specific interactions contained in $\Delta G_{NS}/RT$ have the same additive effect as the concentration [C] on the multivalent binding free energy. As $\Delta G_{NS}/RT$ may be tuned by chemical design in principle, then it is an additional adjustment knob for shifting the value of the surface receptor density where the adsorption inflection point occurs. In practice, most multivalent binding systems have non-specific interactions that are intrinsic in the design -both in human-made and nature-made systems. However, in the following section we will highlight how these interactions can be designed to enhance binding selectivity.

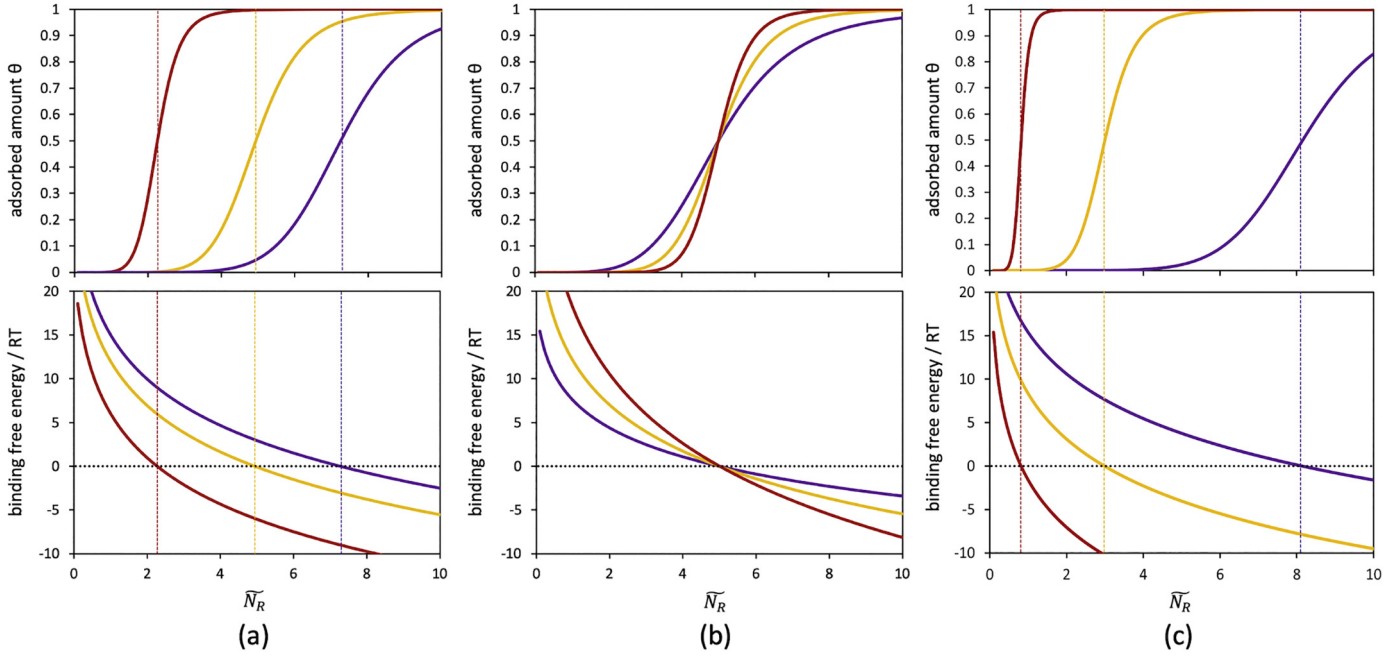

Fig. 3. Multivalent adsorbed amount θ (Eq.4, upper panels) and binding free energy (Eq.2, lower panels) as a function of the number of receptors $\widetilde{N_R}$ per surface area a^2. In (a), the ligand-receptor binding free energy $\Delta G_{lig}/RT = -2$ (a typical value for a weak ligand-receptor bonding interaction) and the number of ligands $\widetilde{N_L} = 8$ are kept fixed. Three particle concentrations [C] ranging over a factor of 10^{12} are shown (purple, yellow, red, from smallest to largest). Vertical dashed lines indicate inflection points for each adsorption profile. In (b), the particle ligand-receptor binding free energy is also fixed at $\Delta G_{lig}/RT = -2$, while the number of ligands on the particle is set to $\widetilde{N_L} = 5$, 8, 12 (purple, yellow, red). In each case, the concentration is adjusted such that the binding transition occurs at $\widetilde{N_R} = 5$. In (c), the particle concentration [C] is fixed and the number of ligands per particle is fixed to $\widetilde{N_L} = 8$, while the ligand-receptor binding free energy is set to $\Delta G_{lig}/RT = -1.5$, -2.5, and –3.8 (purple, yellow, red); this corresponds to varying K_i over a factor of 10.

The molecular design of a multivalent particle controls how sharp (super-selective) its binding transition is. Fig. 3B shows how the sharpness of the adsorption curve may be modulated by changing the number $\widetilde{N_L}$ of ligands per particle. In each case, the concentration of particles in solution has been tuned so that the adsorption transition is centered at $\widetilde{N_R} = 5$. Adding more ligands to each particle (increasing $\widetilde{N_L}$) causes the gradient of $\Delta G_{\text{bind}}/RT$ with $\widetilde{N_R}$ to be steeper and more negative, leading to a sharper binding transition.

Finally, in Fig. 3C, we illustrate how the binding free energy and adsorption profile varies with the ligand-receptor binding strength ΔG_{lig}. Following intuition, a larger ligand bond strength leads the multivalent particles to adhere to surfaces with a lower receptor density, while the inflection point grows sharper.

Comparing panels (a) and (c) of Fig. 3 allows for a general assessment of how relatively sensitive the adsorption profiles are to variations in the concentration [C] and bond strength ΔG_{lig}. In (a), in order to shift the inflection point of the adsorption profile from $\widetilde{N_R}$ near 2 (red) to around 7.5 (purple), the concentration [C] must be reduced by a factor of 10^{12}. This is orders of magnitude below an experimentally-reasonable dilution. While other binding scenarios may differ quantitatively, this example illustrates a more general point: only minimal modulation in the multivalent binding adsorption profile - specifically shifts in the inflection point as a function of target receptor density - may be achieved with a variation of the concentration of the multivalent particles.

On the other hand, if we examine panel (c) of Fig. 3, we find that almost the same shift in the position of the adsorption inflection point can be accomplished with only a factor 10 change in the ligand-receptor binding constant K_i. The reason for this high sensitivity is because the ligand-receptor bond strength ΔG_{lig} is exponentiated inside the logarithmic term in Eq.2, which is subsequently multiplied by the number of ligands $\widetilde{N_L}$ available for bonding. Indeed, in the limit of strong ligand-receptor bonding in Eq.3, the overall binding free energy is linear in ΔG_{lig}. On the other hand, the binding free energy only depends logarithmically on the particle concentration [C].

This sharp dependence of the multivalent affinity on the ligand-receptor binding constant K_i has two consequences. Firstly, it means that the ligand chemistry may be tuned only by slight variations in order to achieve entirely different multivalent targeting profiles. However, this also means that small uncontrolled/undesired variations in the ligand design can lead the desired targeting recipe to "miss its mark" by a large margin. Indeed from the mathematical model, we see that multivalent constructs with more ligands are much more sensitive to small variations in K_i. Thus, concise design of the multivalent construct is essential to success in a desired targeting recipe.

In practice, multivalent constructs often have a non-homogeneous distribution of ligands attached to their surface/core. If the ligands are mobile, then they may freely diffuse on the particle surface, and so their initial placement positions are irrelevant; this is not the case for immobile ligands, however. For example, ligands grafted to fixed positions on the surface of colloidal particles may end up being distributed uniformly, randomly, or in clusters, depending on the grafting methodology and chemical composition of the ligands. The influence of how the ligands are distributed on the surface of a multivalent particle is studied theoretically and computationally for colloidal particles with reversible surface binders [45]. In general, spatial heterogeneity of ligand placement does not *qualitatively* disrupt or eliminate the super-selective multivalent binding physics; however, it does lead to a shift in the inflection point of the super-selective adsorption profile (like those shown in Fig. 3).

2.1.3. How to exploit multivalent design

In the preceding section, the dependence of super-selectivity on the design parameters of multivalent systems was discussed. We now elaborate on these trends in the context of nanomedicine targeting.

Many weak-binding ligands. Particles with a higher ligand density are able to participate in more simultaneous ligand-receptor bonds. This leads to a larger permutation entropy contribution to their binding affinity, and thus a stronger dependence on the density of receptors on the target. Such high-valence multivalent particles are therefore more selective for surfaces with high receptor density, while having low binding affinity for low-receptor-density surfaces.

This effect is contingent on a sizeable permutation entropy contribution to the binding affinity. For example, if the ligands on the multivalent particles are strong-binding, then the entropic contribution becomes small in lieu of a very large binding enthalpy, and this selectivity is reduced. Thus, *weak-binding* ligands are ideal, so that dependence of binding affinity on the surface receptor density is maximized. Good candidates for weak-binding ligands include glycans [105] and peptides [16,106,107]. High binding sensitivity to small variations in surface receptor density is particularly important for targeting cancerous cells, which are typically quite similar to healthy cells in terms of surface receptor density and profile [97].

There is another impact that strong-binding ligands may have. In some cases, the *total* number of receptors on the binding surface is limited. If the receptors are mobile on the surface, e.g. if it is a fluid membrane or vesicle, then few multivalent particles with strong-binding ligands may adsorb to the surface and "recruit" all of these receptors [108,109]. This constitutes a long-lived kinetic regime, wherein the bound ligands must liberate receptors (through thermal fluctuations or otherwise) in order for additional multivalent particles to bind to the surface.

More flexible is more selective. Greater flexibility affords multivalent particles to potentially have more simultaneous ligand-receptor bonds with their target, enhancing their selectivity. Longer and more flexible ligands can bind to more possible receptor partners. In this regard, solid multivalent constructs like spherical nanoparticles or colloids are limited when the particle size is much larger than the individual ligand and receptor size; ligand-receptor interactions are restricted only to the small fraction of the particle surface area that is directly in contact with the target.

An alternative is to use multivalent polymers, which may freely explore different conformations in order to maximize binding interactions with their target [110]. This strategy has been successful in targeting immune cells [111]. However, polymers may also be self-limiting, as inert parts of a bound multivalent polymer can crowd nearby surface area of the target, reducing other particles from binding. More flexible constructs are also more likely to fluctuate their ligands *away* from the receptor surface, such that the effective molarity of receptors (from the perspective of a ligand) is smaller than when the ligand is forced to reside closer to the receptor surface. Intermediate structures between the "solid particle" and "flexible polymer" extremes might therefore present the best selectivity, such as flexible vesicles, semi-flexible rod-like polymers, and two-dimensional sheet-like objects constructed from biomolecules (e.g. DNA origami).

Targeting entire receptor density profiles; binding and endocytosis. Cell surfaces typically have a variety of receptor types, each having a distinct average concentration on the cell surface. This represents a well-defined "profile" of receptors on the cell surface, which may be strategically targeted. Curk *et al.* have shown by theory and coarse-grained simulation that multivalent particles may be constructed to address a particular receptor profile selectively [19]. The best multivalent design is one where: the construct has different types of ligands, which uniquely target each class of particular receptors on the target (referred to as "multiplexed" targeting [53]); the concentration profile of ligands on the multivalent construct match the densities of the different receptor types on the target; and finally, the ligands are weak-binding with their target receptors.

The design of the multivalent particle also impacts its ability to become endocytosed by the cell membrane, discussed at length via coarse-grained simulation [19]. The better the match of the ligand

profile with the receptor profile on the cell surface, the better the success rate of endocytosis. Ligand-receptor bonds that are weak and dynamic promote facile diffusion of the multivalent particle on the cell surface, allowing it to localize at a favorable site for endocytosis while minimizing the chance that it gets thermodynamically or kinetically "stuck" on the cell membrane.

Enhancing selectivity with non-specific interactions, forces, and flows. "Non-specific interactions" comprise any of the additional interactions between the multivalent particle and the target which are not explicitly part of the "multivalent" contribution. These may include how the scaffold of the multivalent construct interacts with the target, how the ligands and receptors interact with the other chemical constructs on the target cell membrane or multivalent particle, charge-charge interactions and steric repulsions. While many of these interactions are a side-effect of the multivalent particle design, some may be employed deliberately in order to enhance targeting selectivity. Recent theoretical work has focused on manipulating selectivity by grafting inert flexible polymers to the surfaces of multivalent particles, akin to a polymer brush. The polymer brush results in extra excluded volume interactions between the particle and the target [53,112,113], yielding a positive (unfavorable) ΔG_{NS} contribution in Eq.2. The reduced non-specific affinity of the multivalent particle to the receptor surface makes its binding more selective to variations in target receptor density.

An additional step to take is to design multivalent particles to "release" their inert polymers only when bound to the target. In this regime, the multivalent adsorption profile approaches an infinitely-sharp "hyper-selective" transition [113]. In practice, triggered uncoiling of the inert polymers on bound multivalent particles could be accomplished by chemical stimulus, either externally induced, or caused by the ligand-receptor binding events themselves.

The inert polymers effectively impose a "force field" when the host multivalent particle approaches a target for binding. Thus, other kinds of external force fields – e.g. magnetic, electric, chemical gradient, or continuous flow of the surrounding medium – may be imposed in order to manipulate selectivity [113] (Flow may also be inevitable, depending on the environment around a cell membrane). A constant force field applied normal to the target surface leads to a sharpening of the adsorption profile, and therefore greater sensitivity to the density of receptors on the potential targets. If the force field can be applied only to bound multivalent particles, then adsorption enters into the above mentioned "hyper-selective" regime.

Enhancing selectivity with competitive multi-species binding. The simple multivalent thermodynamics summarised here provides insight for constructing systems that exhibit more elaborate super-selective binding and self-assembly, often involving one or more competitive binders [114,115]. For example, an equimolar mixture of low-valence particles with strong-binding ligands can compete for binding, onto the same receptor-coated surface, with a high-valence weak-ligand species [51]. This design sets up a thermodynamic competition between the enthalpic and entropic terms in the multivalent binding free energies for the two particle species (Eq.2), depending on the surface receptor density. At low receptor density, the low-valence particles (with the strong individual ligand-receptor bonds) selectively bind to the surface, as the high-valence species neither has strong-binding ligands, nor a large enough ligand/receptor permutation entropy contribution to drive the binding. Increasing the surface receptor density then leads to a sharp super-selective switch-point, after which the surface becomes occupied by the high-valence species. In the latter regime, the permutation entropy dominates the binding free energy, favouring the species that can form the most simultaneous ligand-receptor bonds, even though that are each individually weak.

We have focused on how super-selective multivalent particles preferentially bind to targets with a *high* receptor concentration. However, there are circumstances where it may be desirable to address only surfaces with a *low* receptor density preferentially. For example, myocardial beta-1 receptors are down-regulated in heart failure, and dopamine transporters are reduced in Parkinson's disease [116,117]. The selective targeting of down-regulated receptors may be accomplished with a two-component "attacker and guard" strategy [52]. The guards are monovalent receptor-sized binders that occupy (or "guard") the surfaces with high receptor density, forcing the attackers to bind to (or "attack") the surfaces with low receptor density.

2.2. Understanding cell target expression

A critical step to achieve multivalent nanomedicine targeting is the choice of the target receptor. As seen from the previous discussion on multivalent design, the density and mobility of the target define the design parameters to achieve (super-) selective nanoparticle targeting. One of the strategies proposed to achieve super-selectivity includes targeting a specific receptor expression profile. Multivalent selectivity can be gained by matching the ligand densities on the nanoparticle to the receptor density. Furthermore, a super-selective regime of targeting can be promoted by a maximal difference in receptor expression between the healthy and the diseased cells.

For this purpose, the overexpression of receptors induced by some cancer types can be exploited. For example, 20% of breast cancer tumors are classified as HER2 positive because of their overexpression of the HER2 extracellular receptor compared to the normal breast epithelium (40-100-fold increase) [118,119]. This difference qualifies HER2 as a promising candidate for targeted therapies, as demonstrated by the success of monoclonal antibodies trastuzumab and pertuzumab [120], and paves the way for a promising nanoparticle targeting strategy [121]. In contrast, triple-negative breast cancer – representing 15-20% of all breast cancers – is difficult to target due to its heterogeneity and the lack of a characteristic receptor profile [122], posing a severe challenge to targeted therapies.

We must acknowledge that targeted therapies are not always possible. For example, receptors that do not internalize upon ligand binding are most likely not suitable for nanoparticle targeting, as often active agents encapsulated inside nanoparticles need to reach intracellular targets [123]. Thus, structural biology plays an important part to elucidate the mechanisms of action of cell receptors, as reviewed elsewhere [124–127]. Additionally, the abundance of endogenous ligands might compete with nanomedicine receptor targeting, stressing the importance of cell target choice. Nevertheless, it remains crucial to stratify patients between groups that will benefit from targeted therapies and groups that will be better treated with classical chemotherapies or promising alternative strategies such as immunotherapies [128].

The heterogeneous spatio-temporal receptor expression is an additional challenge when choosing the right target [129]. In space, receptor expression can vary significantly from patient to patient and from cell to cell [83,130] (Fig. 4). For example, cancer cells present high genetic instability and flexibility to adapt to the microenvironment [81,131–133]. In the same tissue, diseased cells that lack the targeted

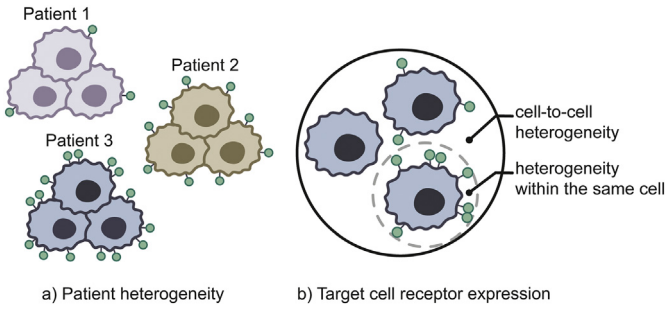

Fig. 4. Schematic representation of cell receptor expression heterogeneity (A) between different patients (B) within the same tissue. (A) Example of 3 different patients expressing 3 different levels of target receptor. (B) Receptor expression levels are heterogeneous from cell to cell or within the same cell.

receptor will not show any therapeutic impact and limit the overall nanomedicine efficacy [24,82]. The receptor organization within the same tissue or cell (Fig. 4B) can change upon clustering of receptors induced by external stimuli. As an example, the EGF receptor family members are prone to form homoclusters (clusters of the same receptor) or heteroclusters (clusters of different receptor members) upon ligand binding [134,135]. This heterogeneity causes some nanomedicines to be only successful in treating a selected number of patients while ineffective for others. In time, cell receptor expression can be highly dynamic due to continuous internalization, recycling, degradation or shedding processes [136–138]. Specifically, these phenomena often occur as a response to ligand binding. [139]. The dynamic nature of receptor expression may jeopardize the targeting strategy and lead to undesired consequences such as off-targeting or low accumulation of nanomedicines at the site of interest.

For the reasons stated above, the oversimplified conception that 'one nanomedicine fits all' should be abandoned. Personalized nanomedicine evolved because of the necessity to choose the right target for the right patient at the right moment [140–146]. To fulfil this necessity, rigorous information about 'where and 'when' the target receptor is expressed is required. For this purpose, quantitative methods to characterize the expression of target receptors are highly desired.

In the next section, we will briefly review current methods that are used in the clinic to quantify receptor expression levels and focus mainly on new quantitative techniques that provide the number or density of receptors. A few representative examples of these techniques will be highlighted, with emphasis to those that aid in the design of multivalent nanomedicines by providing a molecular understanding of the target.

2.2.1. Aiming for the target: quantification of cell receptors

In the clinic, the receptor expression status of patient serves as a marker for the disease outcome and is a standard parameter to decide for a particular therapy. Clinically approved methods to quantify receptor expression can be performed *in vivo* or on a histological sample *ex vivo*. *In vivo* imaging modalities that have enough molecular sensitivity to map cell receptors are positron emission tomography (PET) and single-photon emission computed tomography (SPECT) [147,148]. Even though these techniques provide relevant information and are minimally invasive to the patient, biopsies are often required to extract more detailed information about receptor expression status (heterogeneity, mutations) in tissues. *Ex vivo* tissue analysis is commonly performed using genomic analysis such as sequencing and fluorescence *in situ* hybridization (FISH) or immunohistochemistry (IHC). FISH assesses the gene amplification of receptor genes while IHC reflects the overexpression of a particular receptor. In nanomedicine development, FISH is limited because it lacks information about the true expression of receptors and their spatial distribution. IHC, on the contrary, provides a direct assessment of the number of targets using antibodies attached to a chromogenic reagent (usually an enzyme that converts a soluble substrate into a colored product) (Fig. 5A). However, it is based on a semi-quantitative grading system, thus fails to provide absolute numbers and distribution of receptors.

These limitations triggered the development of more reliable, reproducible and quantitative methods that are currently evaluated for their use in diagnostics. New imaging methods such as spectral imaging, light sheet microscopy and super-resolution imaging emerged in the last ten years as powerful tools for biologists. In particular, super-resolution microscopy is evaluated for the quantification of receptor expression at the cellular and sub-cellular level. Herein we select representative examples of such quantitative techniques that can be applicable for nanomedicine research because they report the number or density of receptors. We first outline representative examples of quantitative single-cell techniques (Fig. 5), followed by the introduction of single-molecule approaches (Fig. 6).

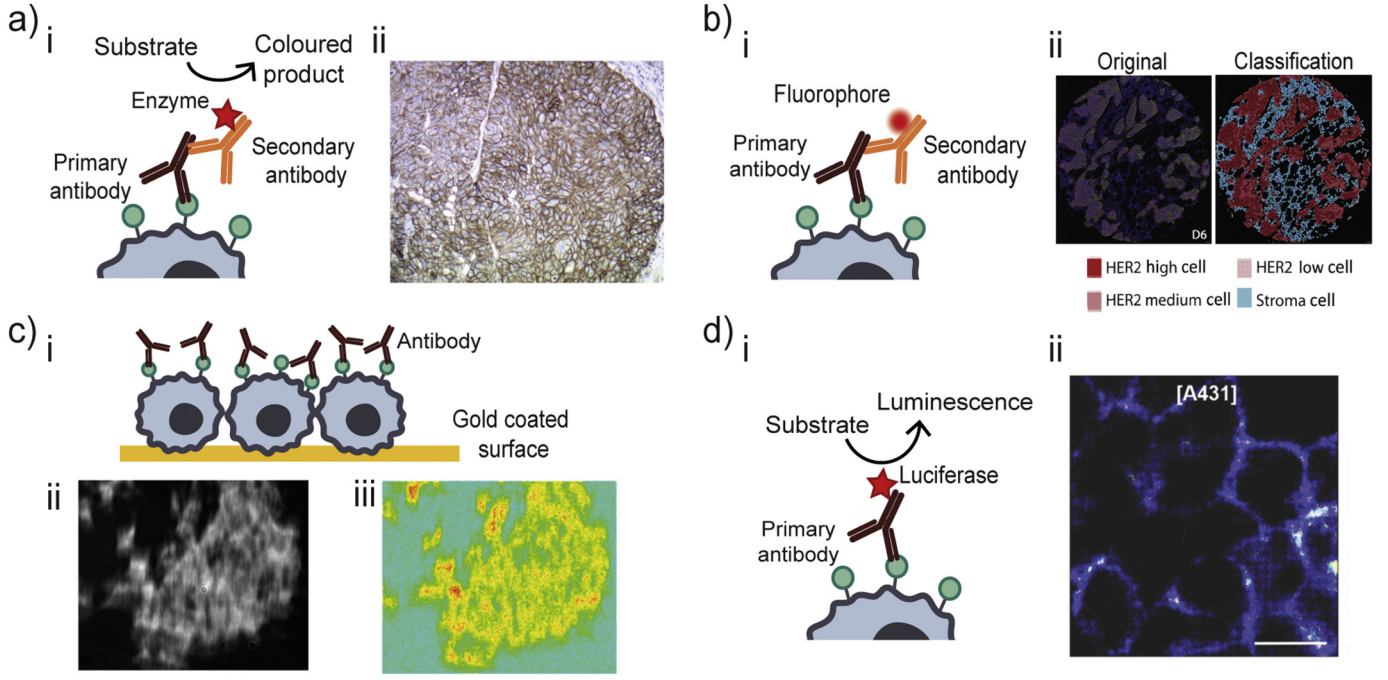

Fig. 5. Selection of quantitative single-cell microscopy techniques for cell receptor expression characterization compared to standard immunohistochemistry. (A) Immunohistochemistry (IHC). (i) Schematic representation of IHC. (ii) IHC staining of EGFR in lung squamous cell carcinoma adapted from [250] under a Creative Commons license[] (B) Quantitative immunofluorescence. (i) Schematic representation of immunofluorescence (IF). (ii) IF staining of breast cancer cells expressing different levels of HER2. Segmentation and classification of cancerous and non-cancerous (stroma) cells were performed quantitatively at a single-cell level. Figure adapted with permission of Elsevier from [152]. (C) Surface-plasmon resonance. (i) Schematic representation of the experimental setup. Cells are seeded on a gold-coated surface for SPR analysis (ii) SPR image of A431 cancer cells before ligand binding. (iii) SPR intensity increase due to ligand binding. Figures (ii,iii) adapted with permission from [155]. (D) Bioluminescent assay. (i) Schematic representation of a bioluminescent assay. (ii) Bioluminescence image of EGFR expression in A431 cancer cells. Figure adapted with permission of Wiley from [156].

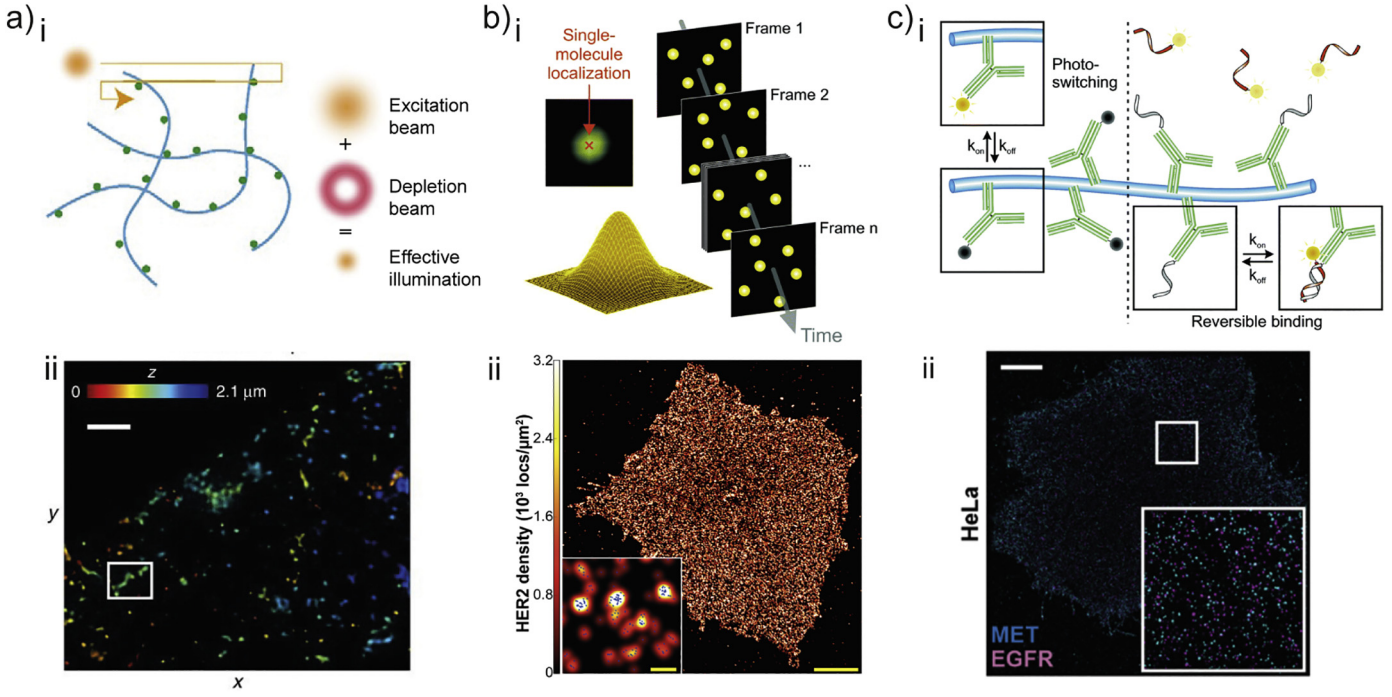

Fig. 6. Selection of quantitative single-molecule microscopy techniques for cell receptor expression characterization. (A) STED. (i) Schematic representation of STED microscopy. The sample is illuminated with an excitation beam and a high-intensity doughnut-shaped depletion beam to selectively turn on fluorophores in the doughnut center. Figure adapted with permission of Elsevier from [186]. (ii) 3D Molecular map of transferrin receptors in HEK293 cells. Figure adapted from [178] (B) Stochastic optical reconstruction microscopy (STORM). (i) Schematic representation of STORM adapted with permission of RSC from [164]. Single molecule blinks are localized and fitted to a gaussian to find the fluorophore center positions. The final image is a reconstruction of thousands of acquired frames (ii) HER2 density in BT-474 cells. Figure adapted from [165]. (C) DNA-PAINT. (I) Schematic representation of DNA-PAINT adapted with permission of RSC from [164]. (ii) MET and EGFR expression in a Hela cell imaged using DNA-PAINT multiplexing. Figure adapted under a Creative Commons license from [185].

Quantitative immunofluorescence builds upon the classical IHC by taking advantage of fluorescence imaging and incorporating automated image analysis and improving the reliability of current protocols. Early work in this area includes the development of automated quantitative analysis (AQUA) to perform high-throughput screening on tissue sections [149,150] and study the heterogeneity of biomarkers in tumours [151]. While AQUA uses a scoring system to categorize biomarker expression, Onsum *et al.* expanded this method to quantify absolute numbers of receptors at a single-cell level [152] (Fig. 5B). The authors quantified the total HER2 expression in fixed tissue samples using fluorescently labelled anti-HER2 antibodies and automated image analysis tools for single-cell resolution.

As seen in the examples above, immunolabeling methods typically require the use of an enzymatic (IHC) or a fluorescent tag (immunofluorescence). In some instances, this results in am more laborious sample preparation. In contrast, surface plasmon resonance (SPR) is a label-free technique than can be used to study ligand binding kinetics and receptor densities [153,154]. In this approach, cells are seeded on a gold-coated surface for analysis. Upon ligand binding, the increase in total mass causes a refractive index change that is recorded in an SPR sensorgram. The SPR intensity change can be correlated to the number of bound ligands (hence the number of receptors) by knowing the mass of one single ligand. Zhang *et al.* used this technique to quantify the EGFR receptor density using an anti-EGFR antibody and gained additional information about its binding kinetics [155] (Fig. 5C).

While the previous methods analyze fixed cells, live cells can be characterized in their native state using a bioluminescence assay. In contrast to fluorescence-based methods, this approach is based on the emission of light produced by an enzymatic reaction (Fig. 5D). As such, it is not limited by photobleaching and presents minimal background signal. Ramji and co-workers attached a luciferase enzyme to an antibody to quantify the number of ß1 adrenergic receptors in cardiomyocytes [156]. The monitoring of the density of these receptors are highly relevant to predict possible heart failures.

For the mentioned methods to be quantitative, a reasonable big sample size needs to be collected for reliable statistics. High-throughput techniques such as fluorescence-activated cell sorting (FACS) have the advantage of a fast, automated and unbiased sample collection. FACS is based on the labelling of biomarkers for expression analysis and cell classification. Thus, it is a suitable technique for single-cell receptor quantification. Quantitative FACS is possible by using commercial beads with different levels of fluorophores attached to define a standard curve. The fluorescent intensity originating from the cell receptor staining can be translated into the number of receptors per cell or receptors per cell area using the standard curve [158–161]. FACS requires suspended cells for its analysis, and therefore, it is mostly used in the field of immunology while it is less suitable to study tissues with adherent cells (e.g. epithelial).

2.2.1.1. Single-molecule techniques. Up to this point, we reviewed methods that characterize the receptor expression at a cellular level. These methods provide valuable insight into the patient-to-patient and cell-to-cell receptor heterogeneity but lack resolution to characterize heterogeneity within the same cell (Fig. 4B). Over the last years, super-resolution microscopy emerged as a new tool in biology, providing molecular detail of cellular organelles and membranes [162]. The resolution is considerably increased compared to conventional fluorescence microscopy by overcoming the diffraction limit of light. Super-resolution microscopy includes several fluorescent-based techniques that accomplish resolution at the single protein level and thus qualify as excellent candidates to quantify receptor expression [163,164]. Examples include the imaging of cancer [165], immune cell [166] or stem cell [167] biomarkers.

Early super-resolution approached used near-field scanning optical microscopy (NSOM) to map the topography of cells. This scanning probe microscopy approach resolves 40-100 nm [168] and was used to characterize the number and distribution of ß-adrenergic receptors and the clustering of EGFR receptors [169,170]. More recent examples of super-resolution microscopy include stimulated emission depletion (STED) and single-molecule localization microscopy (SMLM) [171–175] (Fig. 6). Despite challenges in sample preparation and data analysis, the nanometer resolution provided is unprecedented reaching routinely 20-30 nm and single-digits resolutions in some optimized cases [176].

STED is based on shaping the laser beam to selectively illuminate only a small number of fluorophores at a time. An excitation beam illuminates a selected number of fluorophores while closely adjacent fluorophores are switched off by stimulated emission using a high-intensity doughnut-shaped depletion beam. As a result, only fluorophores in the doughnut centre are excited and imaged. While STED use is limited in live cell imaging due to phototoxicity caused by its high-intensity laser beam, it provides a good resolution (16-80 nm) in fixed cell samples [174]. This enhanced resolution was explored to identify new features in tissue sections which remained hidden using conventional microscopy techniques, demonstrating the added value of STED in clinical diagnostics [177]. Notably, STED can be applied to the molecular counting of receptors. For example, Ta *et al.* applied STED to quantify transferrin receptors in human embryonic kidney cells [178] (Fig. 6A).

In the field of SMLM, two modalities stand out to quantify cell receptors, namely stochastic optical reconstruction microscopy (STORM) and DNA-based points accumulation for imaging in nanoscale topography (DNA-PAINT). STORM makes use of photoswitchable dyes to separate the fluorescent signal of the sample in space, meaning that only a few excited dyes are detected in every image. This spatial separation of fluorescence is perceived as 'blinking' events that are detected and analysed to find the centre position of each fluorophore with high precision. The final image is a reconstitution of all fluorophore positions that are collected over thousands of frames (Fig. 5f (i)). Because it is a single-molecule technique, it facilitates the counting of individual cell receptors. This molecular sensitivity allows the detection of weakly expressed receptors that cannot be detected using conventional techniques such as FACS [179]. A few studies highlight the power of STORM in quantitative receptor determination. Sauer and co-workers first introduced this approach to map the number and organization of the metabotropic glutamate receptor using a fluorescently labelled antibody [180]. In contrast, Dietz *et al.* used fluorescently labelled ligands to quantify the density of receptor tyrosine kinase MET and tumor necrosis factor 1 receptor [181]. In a similar approach, Tobin and co-workers used labelled therapeutic antibody trastuzumab to quantify the density of HER2 receptors in breast cancer cell lines and patient tissue [165] (Fig. 6B).

DNA-PAINT makes use of the reversible and transient binding of complementary DNA strands, one strand being attached to the molecule that recognizes the receptor of interest while the complementary strand is attached to a fluorophore and freely diffuses in solution [182]. A DNA-binding event is visualized as a bright fluorescent spot, and the stochastic binding of DNA-strands to their target is perceived as 'blinking'. Like STORM, the final image is reconstituted by collecting all these binding events over thousands of consecutive frames. Using quantitative DNA-PAINT (qPAINT), Jayasinghe and colleagues revealed the clustering of ryanodine receptors in nanodomains and quantified the number of receptors forming each nanodomain [183]. A clear advantage compared to STORM is the multiplexing ability of DNA-PAINT using different pairs of complementary DNA strands, enabling the characterization of several receptors on the same sample. In line with a multivalent nanoparticle design, the possibility to characterize multiple receptors is a desirable feature to enable multiplexed targeting. The co-localization and clustering of MET and EGFR was investigated upon ligand stimulation using this multicolor modality [184,185] (Fig. 6C).

Overall, this recent advances on the quantification of receptor expression at the molecular level can contribute to an improved understanding of the number of targets. An overview of the discussed quantitative techniques to characterize cell receptors can be found in Table 1. In particular, we have shown that cell-to-cell heterogeneity and cellular distribution can be uncovered by using single-molecule techniques.

2.3. Understanding the functionality of nanoparticles

Quantitative methods for ligand characterization are necessary to understand nanomedicine specificity towards the tissue of interest. In the previous section, we focus on the understanding of the biological targeting terms of number or density of receptors. Next, we aim to achieve a better characterization of our targeting 'bullets'. Together, this information can provide valuable knowledge about the nanomedicine targeting efficiency, affinity and (super-) selectivity towards the target cell population.

Surprisingly, there are no standardized characterization methods of nanoparticles before entering clinical testing [4]. A series of guidelines named MIRIBEL (Minimum Information Reporting in Bio-Nano Experimental Literature) were recently proposed to standardize bio-nano research across laboratories [93,188]. To the best of our knowledge, this is the first attempt to improve the reproducibility in the field, providing concrete examples to turn qualitative into quantitative research.

Like cell receptor expression, nanomedicines can be very heterogeneous in terms of the number of ligands (Fig. 7A). However, nanoparticles are a hundred times smaller compared to cells, which presents technical challenges to understand this heterogeneity at a single particle level. Thus, most measurements are performed in bulk or ensemble, and average numbers are reported. Although the effects of ligand density on targeted nanoparticles in cell experiments or *in vivo* are often reported [95], the majority of these findings lack quantitative methods to characterize the number of targeting ligands, let alone the single-particle heterogeneity [84]. Targeting ligand may vary in composition and sizes (antibodies, peptides, aptamers, sugars, and other small molecules [189]), but the general discussion presented in this section applies to all of them.

In the context of multivalent design parameters, we have shown that a subtle change in the number of ligands can modulate the super-selective binding transition of nanoparticles in the right conditions. The main problem we are facing is that standard conjugation methods are often nonselective and lack in control of ligand number and orientation (Fig. 7A,B). For example, antibodies have two antigen-binding sites which can be totally, partially or non-accessible for target recognition depending on how they orient on the nanoparticle surface [190] (Fig. 7B). A mixture of good and badly oriented antibodies can result from random conjugation methods, such as physical adsorption or carbodiimide-based covalent conjugation. However, target recognition can be compromised when bad orientations are favored [191,192]. This scenario illustrates how even a high total conjugation efficiency does not necessarily result in a high ligand functionality. Recent approaches focus on making nanoparticle functionalization more selective [193–195], thus promoting a correct orientation of targeting ligands for their intended application. The control over the ligand orientation is a promising feature, but it remains uncertain whether targeting ligands preserve their functionality after the conjugation reaction.

Ligand functionality can decrease due to denaturation or shielding of the antigen-recognizing sites (Fig. 7C). Ligands such as antibodies or proteins are susceptible to denaturation during conjugation due to hydrophobic interactions with the nanoparticle's surface [89,196]. A reduction in alpha-helix content in human serum albumin attached to nanoparticles was found compared to the protein alone using circular dichroism [197]. Moreover, shielding of binding sites can occur because of ligand crowding [198] or protein corona formation [69]. In the latter case, many efforts have focused on making nanoparticles 'invisible' to

Table 1
Advantages and limitations of quantitative techniques for the characterization of cell receptor expression.

Techniques	Advantages	Limitations	Target
Automated quantitative immunofluorescence	• High throughput • Multiplexing	• Fixed cells • Limited resolution	HER2 [152]
Surface plasmon resonance	• Label free • Quantification of binding kinetics	• No multiplexing • Limited resolution	EGFR [155]
Bioluminescent assay	• Low background signal • Live cell • No photobleaching	• Semi-quantitative • No spatial information • No multiplexing • Limited resolution	EGFR and β1 adrenergic receptor [156]
Fluorescence activated cell sorting (FACS)	• Live cell quantification • High throughput • Multiplexing	• Lack of spatial information • Limited sensitivity	EpCAM [158], EGFR [158], CD44 [158], HER2 [158,160], N-cadherin and E-cadherin [158], α1β3 integrin [158], ICAM-1 [158], ER-alpha [158], VEGFR [159], Neuropilin-1 [159], CD16b [187]
Near-field scanning optical microscopy (NSOM)	• Good resolution (x-y: 40-100 nm)	• Long scan times • Complicate instrumentation	B-adrenergic receptor [169], EGFR [170]
Stimulated emission depletion (STED)	• Relatively large field of view (μm range) • Relatively fast (seconds) • 3D imaging possible • Good resolution (x-y: 50 nm)	• High laser power required • Photostable dyes required • Expensive and complicated instrumentation	Transferrin receptor [178]
Single molecule localization microscopy (SMLM) : STORM, DNA-PAINT	• Excellent resolution (x-y: 20 nm) • Single-molecule visualization and counting • Multiplexing	• Difficult sample preparation • Difficult data analysis • Relatively long acquisition (minutes) • Live cell imaging nearly impossible	Metabotropic glutamate receptor [180], MET receptor [181,184,185], TNF-R1 [181], HER2 [165], Ryanodine receptor [183], EGFR [184,185]

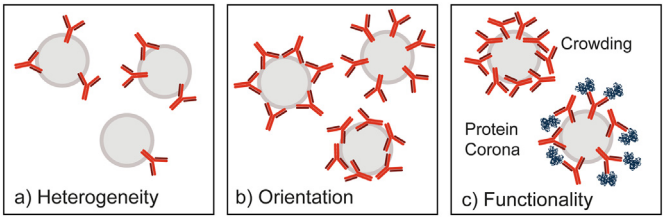

Fig. 7. Schematic representation of targeting challenges at the nanoparticle level. Antibodies (red) are illustrated as a representative targeting ligand. (A) Conjugation methods lead to a significant inter- and intrananoparticle ligand heterogeneity. (B) Random conjugation methods can lead to a variety of ligand orientations on the nanoparticle surface. (C) The functionality of ligand conjugated nanoparticles can be compromised by surface crowding of too many ligands and shielding after protein corona formation.

the biological environment to avoid these undesired effects by coating their surface with hydrophilic polymers (such as poly(ethylene glycol) [199]) or zwitterionic moieties [200]. However, it is still to be determined to what extent these coatings help in preserving the ligand functionality. The sum of these unfavorable processes can lead to the partial or total loss of the ligands functionality [196].

Herein, we discuss quantitative methods to characterize the total and functional amount of conjugated targeting ligands. Characterizing the total amount of ligands on nanoparticles gives us an idea about the success of the conjugation procedure and enables the comparison of different methods. Various methods are described for the characterization of inorganic nanoparticles [201]. However, most of them are unsuitable for organic or polymeric materials. For example, nanoparticle properties play a critical role in techniques such as surface plasmon resonance. The methods described here focus on the characterization of organic nanoparticles (such as dendrimers, liposomes, micelles, polymeric nanoparticles, amongst others) or are potentially applicable to them. A clear distinction will be made between ensemble and single-particle techniques. The latter has a clear advantage in the limit of detection one can expect to reach. Up to date, limited techniques are described to characterize nanomedicines individually, putting microscopy-based techniques into the focus of our discussion.

2.3.1. How many? Characterization of total targeting ligands

A variety of methods have been reported to quantify the number of total targeting ligands conjugated to nanoparticles. The number of total ligands should not be confused with the number of functional ligands, which will be the topic of discussion of the next section (2.3.2).

The total number of conjugated ligands can be determined by indirect or direct methods. By far, the most prominent example of an indirect method is the supernatant assay. This assay is a fast and straight forward method that relies on the quantification of unbound targeting ligands. The amount of ligands in the solution is measured before and after conjugation and the difference is attributed to the effectively conjugated ligands. Native or fluorescently labelled ligands of interested can be measured using UV-Vis or high-performance liquid chromatography (HPLC) [202], biochemical (such as Bradford, bicinchoninic acid (BCA) or enzymatic assay [203]) or immunoassays (for example dot blot immunoassay [204]). The main drawback of this indirect technique is the overestimation of conjugated ligands, due to the loss of ligands in the nanoparticle purification steps [205].

In contrast, direct characterization techniques quantify the number of ligands conjugated to nanoparticles, resulting in a more reliable measurement. Ensemble methods are generally fast and high throughput methods to characterize ligand-functionalized nanoparticles. However, they are based on average values which mask the true heterogeneity of a nanoparticle population. Single-molecule characterization techniques enable the study of individual nanoparticles. Thanks to this

unique feature, heterogeneities in the number of ligands are revealed in the same nanoparticle batch. The main limitation of these techniques is their low-throughput compared to ensemble techniques and the requirement of specialized instrumentation.

2.3.1.1. Ensemble methods for direct ligand quantification. Direct biochemical assays have been described to characterize protein-conjugated nanoparticles. Most of these assays are based on the reaction with proteins to form a measurable colored product. Functionalized nanoparticles can be incubated directly with some of this reagents to quantify the number of ligands attached [206,207]. However, some materials are reported to interfere in biochemical assays such as BCA assays [208]. Small non-protein ligands can also be measured by using a modified protocol. For example, the amount of folate conjugated on PLGA-PEG nanoparticles was determined by detecting the folate molecules with anti-folate antibodies, and the detection antibodies were quantified with a BCA assay [209]. Small peptides are more challenging to quantify because of their reduced number and a limited variety of amino acids. To overcome this limitation, colorimetric assays are available that are based on the interaction with specific functional groups producing a high fluorescent signal. For example, 9,10-phenanthrenequinone reacts with arginine while epicocconone and fluorescamine both react with primary amines. These compounds were used for the quantification of RGD peptides in PLGA-PEG nanoparticles and the binding of nanoparticles to a large panel of proteins [209–212].

Enzyme-based methods can be applied to quantify the number of nanoparticle ligands, besides their standard application in IHC to image cell receptors. Similar to the previous examples, enzyme-based methods are based on the detection of a colored product. Unlike a chemical reaction, the colored product originates in this case as a result of an enzymatic reaction. Enzyme-based methods allow the quantification of ligands using either an indirect or direct approach. Bouzas-Ramos and co-workers reported an indirect method to quantify the conjugation of ligands to streptavidin-functionalized particles relying on the detection of non-conjugated streptavidin sites [213]. In a direct approach, Colombo and co-workers transferred antibody-conjugated nanoparticles onto a blotting membrane to detect the total number of ligands [214].

2.3.1.2. Single-particle methods for direct ligand quantification. HPLC is a direct quantification method that uses a pressurized column to separate nanoparticles according to their number of ligands. This technique is limited to small nanocarriers (for example dendrimers), as bigger particles might block the HPLC columns. Mullen and co-workers used HPLC to obtain information about interparticle ligand heterogeneity in dendrimers functionalized with two different methods [215](Fig. 8). Although the two tested formulations have nearly the same mean number of ligands per nanoparticle, their ligand distributions in Fig. 8 (a) and (b) are very different. This example clarifies that reporting the mean number of ligands is not representative of the true nanoparticle heterogeneity generated after ligand conjugation [87,192].

Single-molecule fluorescence microscopy is a versatile and thus attractive tool to quantify nanoparticle ligands. Two techniques will be highlighted here, namely single-molecule photobleaching and STORM (Fig. 9). Single-molecule photobleaching measures the photobleaching steps of a fluorescently labelled sample to determine the number of total molecules per nanoparticle, with each bleaching step representing a single fluorophore. Nanoparticles can be characterized by fluorescently labelling the targeting ligands and quantifying the number of bleaching steps [216,217]. One of the main challenges is the identification of each discrete bleaching step, which limits this method to low labelling densities [218]. Belfiore *et al.* quantified the number of fluorescently-labelled proteins conjugated to liposomes counting photobleaching steps using total internal reflection fluorescence (TIRF) microscopy [219]. Recently, SMLM has emerged as a powerful tool to characterize the structure of nanomedicines, thanks to its molecular specificity and multicolour possibility [220]. SMLM resolves features of nanomaterials that cannot be visualized using conventional fluorescence microscopy techniques [221]. For example, Feiner Gracia *et al.* studied how the degradation of silica nanoparticles affects the total amount of conjugated antibodies using STORM [85].

Single-particle techniques are a valuable tool for the accurate characterization of nanoparticles. In specific, we highlight the ability of these methods to unveil nanoparticle heterogeneities, which remain uncovered by ensemble techniques. An overview of direct quantification of total nanoparticle ligands (ensemble and single-particle) can be found in Table 2.

2.3.2. How functional? Target recognition ability of nanoparticle ligands

The characterization of the total amount of ligands alone fails to provide information about the functionality of conjugated ligands. Understanding the functionality of ligands is vital to quantify target-recognizing ability and multivalent binding effects, as outlined earlier. Common processes such as denaturation and steric hindrance between targeting moieties reduce the targeting functionality of the nanoparticle significantly. Thus, it is important to understand both the total conjugated ligand and the functional binding sites to modulate nanoparticle functionality [194]. Similar to the previous section, functional ligand

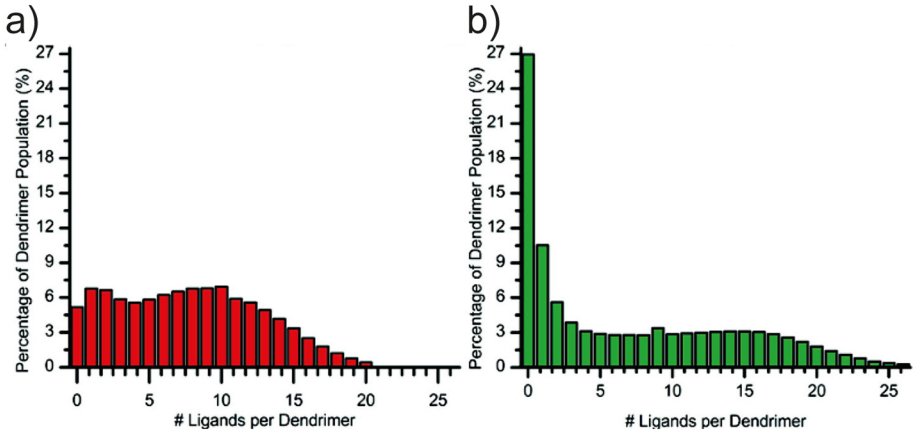

Fig. 8. Distributions of ligand-functionalized dendrimers measured using HPLC. The two formulations despicted in (A) and (B) have a similar mean number of ligands but their distribution if fairly different. The mean number of ligands masks the underlying heterogeneity in these samples. Figure adapted with permission from [215], Copyright (2010) American Chemical Society.

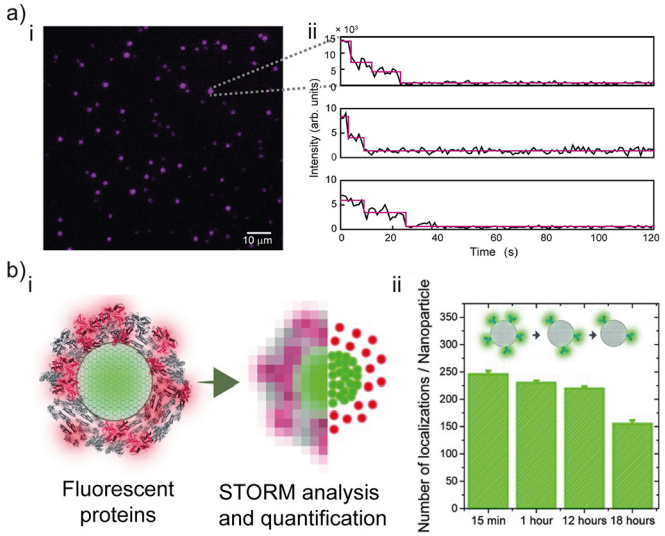

Fig. 9. Single-molecule microscopy approaches to quantify the number of total nanoparticle ligands. (A) Single-molecule photobleaching. (i) Total internal reflection fluorescence image of fluorescently labelled individual proteins. (ii) Example of intensity profiles of single proteins. The individual steps represent bleaching of a single fluorophore. Nanoparticle ligands can be quantified by counting the total bleaching steps. Figure adapted from [219], Copyright 2018, with permission from Elsevier. (B) Stochastic optical reconstruction microscopy (STORM). (i) Schematic representation of STORM quantification. Proteins are fluorescently labelled and counted at a single-molecule bases. (ii) Quantification of number of antibodies attached to nanoparticles in time. Figure adapted with permission of Wiley from [85].

characterization techniques will be divided in ensemble and single-molecule approaches.

2.3.2.1. Ensemble methods for functional ligand quantification. The majority of ensemble methods focus on the characterization of functional antibodies (Fig. 10). As previously mentioned, those can be oriented in many different configurations on the nanoparticle surface. Antibody functionality assays can be performed by either detecting the antigen-binding site (fab) using detection molecules (such as anti-fab antibodies) or in a more direct approach by quantifying ligand binding. In the first case, functional antibodies can be detected using fluorescently-labelled fab-specific antibodies and quantified using UV-vis [226] or flow cytometry [227]. While UV-vis is straight forward to perform, quantification by flow cytometry is limited to particles of a minimum size of 200-500 nm for accurate detection. Lo Guidice and co-workers developed an approach to circumvent this limitation by measuring various nanoparticles simultaneously in a defined volume. Previous knowledge about the concentration of nanoparticles and the detection volume of the flow cytometry laser is required. The authors detected functional transferrin molecules on nanoparticles and reported that only 24-30% of the conjugated transferrin ligands were functional [228].

A direct approach was introduced by Jeong and co-workers, who used fluorescently labelled HER2 antigens to detect functional antibodies coupled to silica nanoparticles. The fluorescent signal of bound antigens was quantified using a fluorescence imaging system. The authors reported that almost full functionality of antibodies was maintained using a controlled click chemistry approach [229]. Saha and colleagues used a sandwich assay to characterize the antigen-binding site and fragment crystallizable region (Fc) accessibility of antibody-conjugated magnetic nanoparticles based on radioactivity detection. This thorough study determined the optimal conjugation parameters for the conjugation of antibodies to nanoparticles but concluded that only between 20-30% of all Fab and Fc fragments were accessible [230]. In a different approach, Lo Guidice and co-workers used immuno quantum dots and fluorescence spectroscopy to detect functional epitopes [231]. In line with the previous results, the authors reported that less than 20% of the conjugated ligands were functional.

Enzyme-linked immunosorbent assay (ELISA) is an easy and commonly used technique in diagnostics [233] and can be applied to characterize active antibodies on nanoparticles. In this approach, antigen or capture molecules are immobilized on microplate wells and incubated with ligand-conjugated nanoparticles. The detection of captured nanoparticles is usually performed using immunoperoxidase or peroxidase conjugates and a substrate that gives a colorimetric signal upon reaction. Using this method, Byzova *et al.* reported that more antibody coverage does not necessarily lead to an increase in active antibodies, indicating that crowding effects play a significant role in the antigen-recognizing ability of antibody functionalized gold nanoparticles [198]. In a similar approach, this method was applied to recognize in the same assay functional antibodies and Fc domain exposure [222]. Enzyme-based methods were also performed in solution using an adapted protocol. However, the reported studies are specific for anti-HRP antibodies. The translation into other targeting ligands might be difficult since only a limited number of antigens have an enzymatic activity that can be used as a readout. Recent reports suggest that covalently-conjugated and protein A-mediated conjugation of antibodies result in more functional nanoparticles compared to physically adsorbed antibodies [194,223]. In another study, it was found that a high amount of conjugated antibodies lead to a decrease in antigen recognition, which can be attributed to steric hindrance among antibodies themselves [224]. Ruiz *et al.* highlighted the importance of pH in the orientation of adsorbed antibodies, suggesting that the positive antibodies charges are responsible for dictating the orientation on the gold nanoparticles surface [225]. These examples stress the importance of studying both the total and the functional number of ligands.

Table 2
Advantages and limitations of total nanoparticle ligand quantification methods. Methods are divided into ensemble and single-particle techniques.

	Advantages	Limitations	Reference
Ensemble techniques			
Supernatant assay	• Fast • easy	• Indirect method • Overestimation of ligands	[202–204]
Biochemical colorimetric assays	• Fast • Specificity	• Nanoparticle interference • Limited in most cases to protein detection	[206,207,209,210]
Enzyme-based methods	• Fast • Cost-effective • Versatile	• Requires detection molecules with enzymatic activity	[213,214]
Single-particle techniques			
High-performance liquid chromatography (HPLC)	• Good sensitivity	• Limited to very small particles	[87,215]
Stepwise Photobleaching	• Versatile • Relatively simple	• Limited to low fluorescent density • Fluorescence quenching	[216,217,219]
Stochastic optical reconstruction microscopy (STORM)	• Molecular specificity • Excellent resolution	• Photobleaching • Difficult sample preparation	[85]

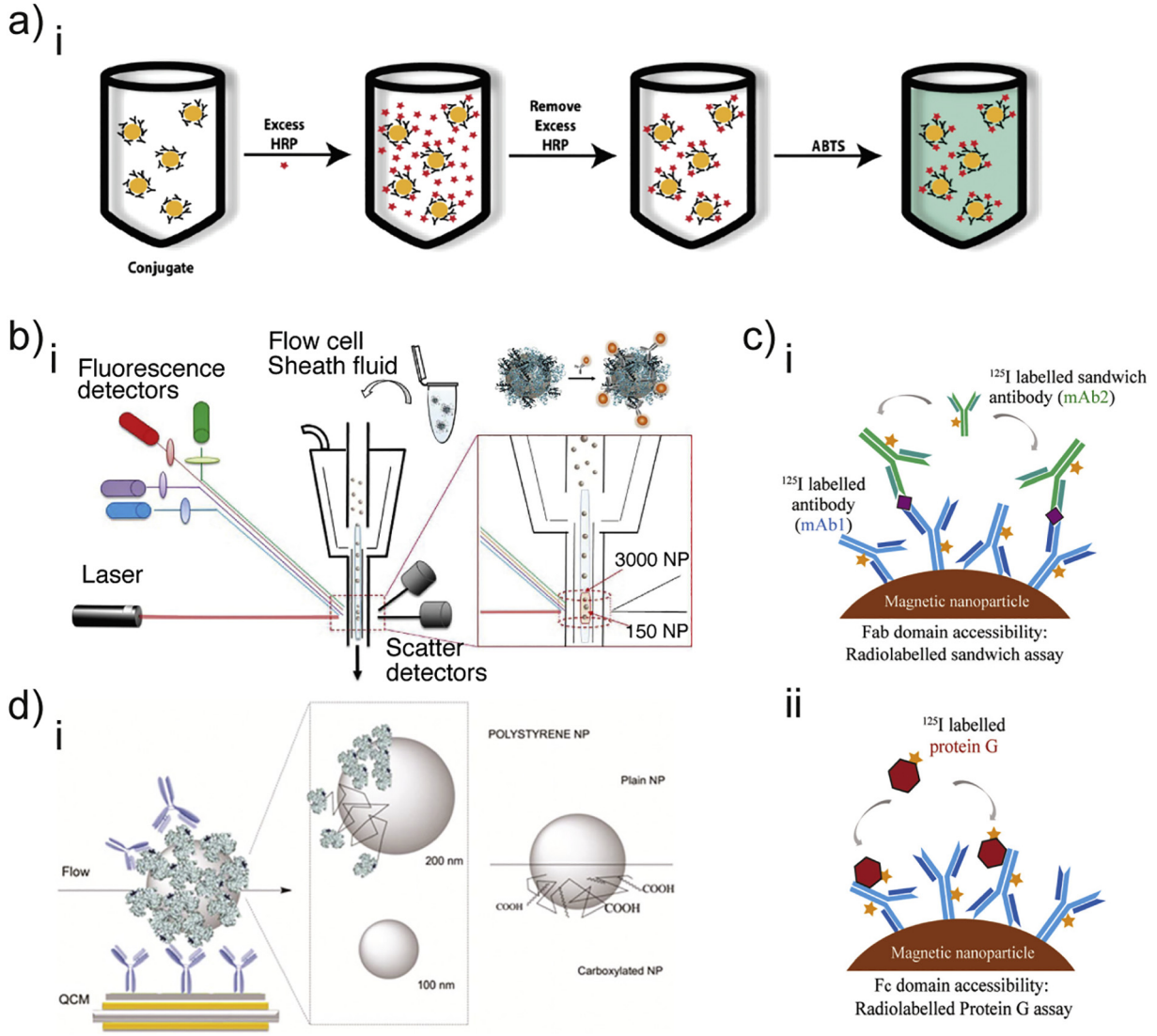

Fig. 10. Selection of quantitative ensemble methods to characterize functional of ligand-conjugated nanoparticles. (A) Schematic representation of an enzyme-based assay performed in solution. Anti-horseradish peroxidase (HRP) antibody conjugated nanoparticles are incubated with HRP to detect the functional ligand binding sites. HRP oxidizes its substrate ABTS resulting in a colorimetric output that can be correlated with the number of functional antibodies. Figure adapted from [225], Copyright (2019) Americal Chemical Society. (B) Schematic representation of fluorescence-activated cell sorting (FACS). Nanoparticles are simultaneously illuminated in a defined volume. Functional nanoparticles can be quantified having previous knowledge about the nanoparticle concentration and the detection volume of the instrument. Figure adapted from [228]. (C) Schematic representation of a radio-labelled assay. (i) Detection of functional antigen binding sites is performed via a sandwich assay. (ii) Detection of fc domains using radio-labelled fc-binding protein G. Figure adapted under a Creative Commons license from [230] (D) Schematic representation of quartz crystal microbalance (QCM) detection. Functionality of nanoparticles is assessed by recording the increase of mass after ligand binding using a quartz crystal resonator. Figure adapted with permission of RSC from [232].

Quartz crystal microbalance (QCM) is a precise and versatile method that detects the change of mass in a system by recording a frequency shift in a quartz crystal resonator. Functionality of nanoparticles can be assessed using the mass shift originating from ligand binding to their antigen [232,234]. Gianneli *et al.* used a sandwich-like approach principle to characterize the functional transferrin ligands on nanoparticles. The authors report a difference in functional transferrin molecules depending on the nanoparticle surface chemistry, remarking that orientation of ligands strongly depends on the nanoparticles nature and should be analyzed carefully in each case [232].

2.3.2.2. Single-particle methods for functional ligand quantification. Single-molecule microscopy approaches have been described to characterize the functionality of ligands on individual nanoparticles. These techniques -mostly based on immunogold electron microscopy or super-resolution fluorescence microscopy- unveil the true heterogeneity of the nanoparticle populations by measuring their ligand functionality (Fig. 11). However, they are generally low throughput and labour intensive, since an adequate sample size needs to be imaged for significant statistics. Transmission electron microscopy (TEM) maps the functional epitopes of ligand-conjugated nanoparticles using a gold nanoparticle probe. Dawson *et al.* reported a consistent low functionality of ligands (1-10%) such as transferrin of epidermal growth factor and a high interparticle heterogeneity [231,235]. Oliveira and co-workers found that covalent conjugation leads to higher ligand binding compared to physical adsorption using both TEM and fluorescence detection of anti-fab antibodies [226]. In the field of SMLM, a novel approach was proposed to quantify the number of functional antibodies on nanoparticles based on DNA-PAINT. Delcanale *et al.* used biotin-DNA probes to quantify the number of functional anti-biotin antibodies conjugated to polystyrene nanoparticles by qPAINT. Consistent with previous single-molecule studies, the authors revealed significant heterogeneity in the nanoparticle populations [236].

In this section, we focused on the investigation of the functionality of nanoparticles in terms of target-recognizing ligands, in contrast to only

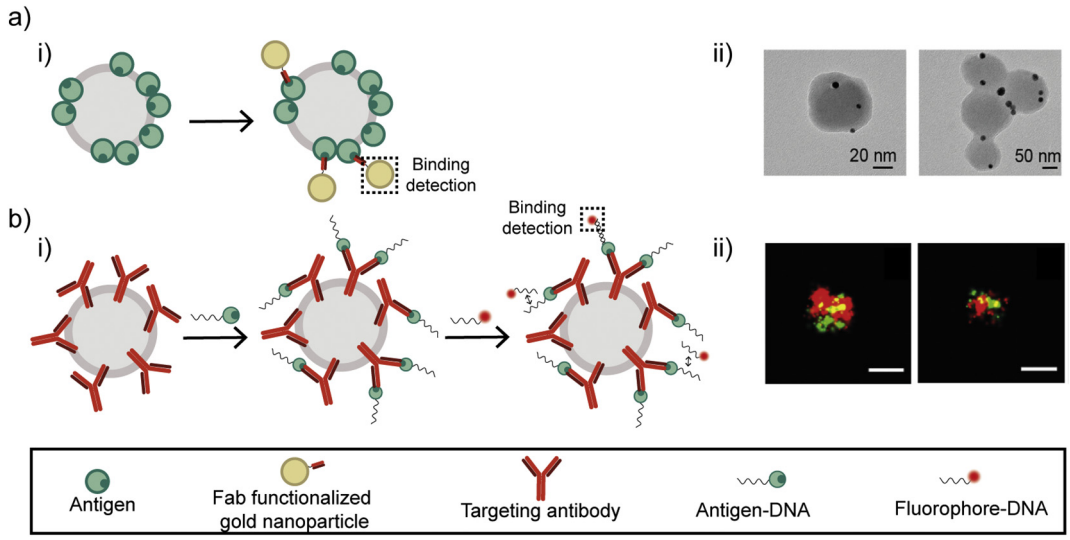

Fig. 11. Single-molecule techniques to quantify ligand functionality on nanoparticles. (A) Antigen epitope mapping using transmission electron microscopy (TEM). (i) Schematic representation of antigen mapping using gold nanoparticle probes functionalized with an antigen binding fragment (fab). (ii) TEM images of the functional epitopes on transferrin-conjugated nanoparticles. Gold nanoparticles are seen as electron dense black spots. Figure adapted with permission of ACS from [235]. (B) Antigen binding site mapping of antibodies using DNA-points accumulation for imaging in nanoscale topography (DNA-PAINT). (I) Schematic representation of DNA-PAINT. Antigen conjugated to a single DNA-strand is used to recognize the antigen binding sites of antibodies conjugated to nanoparticles. Bound antigens are imaged using a fluorophore conjugated to the complementary single DNA strand. (ii) 2-colour DNA-PAINT images revealing functional anti-digoxigenin (green) and anti-biotin (red) antibodies. Figure adapted from [236], Copyright (2018) Americal Chemical Society.

the total number. A summary of functionality characterization methods can be found in Table 3. Surprisingly, we learned that the percentage of functional ligands is relatively low compared to their total number. Once more, we outline that single-particle methods allow investigating the individual heterogeneity of nanoparticles.

3. Future directions and conclusions

Despite the exponentially growing research efforts in the field of targeted nanomedicines, there is no clinically approved therapy so far. This disillusionment demonstrates that targeting is not as easy as postulated in the 'magic bullet' concept more than a hundred years ago by Paul Ehrlich. Therefore, a more profound and quantitative understanding of nanomedicine targeting is needed. Nanomedicine is an interdisciplinary field which requires know-how on many research areas: theoretical modelling, cell biology, chemistry and microscopy, amongst others. We believe that by unifying theoretical prediction and standardized experimental nanomedicine characterization the community can move the field away from a 'trial and error' routine and reach a (more) rational design of nanomedicines.

In this review, we highlight the advances in the theoretical design of super-selective multivalent nanoparticles and quantitative techniques to uncover the real picture of targeting at the cell and nanoparticle level. These two aspects are, in our view, very connected. While modelling can provide a prediction of the most effective design, we need quantitative data to provide input to such a model. In particular, data about receptor expression and mobility, nanoparticle size and number of functional ligands is necessary to match the theoretical predictions.

Table 3
Advantages and limitations of functional nanoparticle ligand quantification methods.

	Advantages	Limitations	Reference
Ensemble techniques			
Fluorescence-activated cell sorting (FACS)	• Fast • Multiplexing	• Nanoparticle size limitation (> 300-500 nm) • Fluorescence quenching	[228]
Radio-labelled assay	• Fast • High sensitivity	• Requires safety measures • Relatively expensive	[230]
Fluorescently labelled antigen detection	• Fast and easy to perform • Versatile	• Unspecific binding • Labelling of antigen required • Fluorescence quenching	[229]
Enzyme-based methods	• Fast and easy to perform • Cost-effective • Versatile	• Requires detection molecules with enzymatic activity	[194,198,222–225]
Quartz crystal microbalance (QCM)	• Versatile • Label free • In flow conditions: mimics in vivo environment	• Steric hindrance between nanoparticles limits detection	[232]
Single-molecule techniques			
Transmission electron microscopy (TEM)	• Label free • Mapping of single-particle functionality	• Labor-intensive • No multiplexing • Dry sample and high vacuum	[226,231,235,237,238]
DNA-points accumulation for imaging in nanoscale topography (DNA-PAINT)	• Multiplexing • No photobleaching • Excellent resolution	• Unspecific DNA binding • Long imaging time • Difficult sample preparation	[236]

Therefore, the availability of suitable characterization methods is a mandatory step towards the controlled formulation of successful nanoparticles, as discussed extensively in this review.

Advances in theoretical modeling highlight the importance of a careful design of targeted nanomedicines to selectively reach a specific cell population. Super-selectivity is an attractive concept that has been intensively studied in theoretical models, but is not yet consolidated in experimental targeting conditions. One of the main challenges to translate theoretical to experimental observations might be the complex implementations of *in vitro* or *in vivo* conditions in current models. We envision that in the future, concepts such as kinetic barriers, the effect of physiological fluids on the binding thermodynamics or competition binding of endogenous ligands with multivalent nanoparticles will improve the understanding and limitations of super-selectivity in a more realistic scenario.

We find that targeting is a *molecular* problem and has to be addressed with techniques able to unveil information at the single-molecule level. The power of single-molecule techniques lies in the uncovering of the underlying heterogeneity in receptor expression and ligand functionalization. Heterogeneity can lead to a broad distribution in functional targeting ligands, which can be advantageous or unfavorable depending on the specific situation. If the receptor distribution on the target cells is equally heterogeneous, this can result in an advantage because more than one cell population is targeted. In contrast, if the receptor distribution is narrow, only a small fraction of nanoparticles will bind specifically, resulting in an overall decrease of targeting efficiency. The presence of this heterogeneity might lead to unexpected consequences and requires further investigation. The ability to count individual molecules opens the door towards understanding and manipulating targeting at a molecular level, instead of relying on semi-quantitative trends. Additionally, we would like to encourage the characterization of ligand functionality as opposed to report ligand numbers solemnly.

The field of optical imaging experienced in the last decade, several breakthroughs and new imaging methods and modalities are now available [239–241]. In particular, super-resolution microscopy can provide molecular quantification of both cell receptors and targeting ligands. The field of targeted therapies can highly benefit of these methods in order to obtain a deeper understanding of both the targeted receptors and the targeting nanoparticles. In general, characterization trends are going towards the combination or correlation of techniques, such as correlative super-resolution and electron microscopy [242]. Correlative light electron microscopy (CLEM) unifies the best characteristics of both techniques and will enable the understanding of new exciting features in the context of individual cellular compartments [243,244].

In the bigger picture, it is crucial to understand and overcome biological barriers that hinder the interaction of nanomedicine with the target receptor (protein corona, cell barriers and extracellular matrix diffusion, amongst others [63,64,71,78,79]). In addition to the approaches highlighted here, methodologies for the quantitative analysis of nanoparticle uptake might help to shed light into the many remaining questions about the nanoparticle fate [245–248]. Together, these efforts and the standardization of quantitative approaches [93,249] will ultimately enable the translation of multivalent nanomedicines from bench to bedside.

In this review, we aim to provide the community with a useful overview of the toolbox for the advancement in the rational design of multivalent nanomedicines. Learning from the current poor clinical success of active-targeted nanoparticles will help us to devise what new fundamental knowledge is needed to design the next generation of targeted therapies.

Acknowledgements

The authors thank the Nanoscopy for Nanomedicine group and the Self-Organizing Soft matter group for the fruitful discussions and feedback. This work was financially supported by the by the Generalitat de Catalunya (2017 SGR 01536), the European Research Council (ERC-StG-757397) and the Netherlands Organisation for Scientific Research (NWO VIDI Grant 192.028).

References

[1] S. Hua, M.B.C. de Matos, J.M. Metselaar, G. Storm, Current trends and challenges in the clinical translation of nanoparticulate nanomedicines: pathways for translational development and commercialization, Front. Pharmacol. 9 (2018) 790, https://doi.org/10.3389/fphar.2018.00790.
[2] J.J. Lee, L. Saiful Yazan, C.A. Che Abdullah, A review on current nanomaterials and their drug conjugate for targeted breast cancer treatment, Int. J. Nanomedicine 12 (2017) 2373–2384, https://doi.org/10.2147/IJN.S127329.
[3] Y. (Chezy) Barenholz, Doxil® — the first FDA-approved nano-drug: lessons learned, J. Control. Release 160 (2012) 117–134, https://doi.org/10.1016/j.jconrel.2012.03.020.
[4] B. Pelaz, C. Alexiou, R.A. Alvarez-Puebla, F. Alves, A.M. Andrews, S. Ashraf, L.P. Balogh, L. Ballerini, A. Bestetti, C. Brendel, S. Bosi, M. Carril, W.C.W. Chan, C. Chen, X. Chen, X. Chen, Z. Cheng, D. Cui, J. Du, C. Dullin, A. Escudero, N. Feliu, M. Gao, M. George, Y. Gogotsi, A. Grünweller, Z. Gu, N.J. Halas, N. Hampp, R.K. Hartmann, M.C. Hersam, P. Hunziker, J. Jian, X. Jiang, P. Jungebluth, P. Kadhiresan, K. Kataoka, A. Khademhosseini, J. Kopeček, N.A. Kotov, H.F. Krug, D.S. Lee, C.-M. Lehr, K.W. Leong, X.-J. Liang, M. Ling Lim, L.M. Liz-Marzán, X. Ma, P. Macchiarini, H. Meng, H. Möhwald, P. Mulvaney, A.E. Nel, S. Nie, P. Nordlander, T. Okano, J. Oliveira, T.H. Park, R.M. Penner, M. Prato, V. Puntes, M. Rotello, A. Samarakoon, R.E. Schaak, Y. Shen, S. Sjöqvist, A.G. Skirtach, M.G. Soliman, M.M. Stevens, H.-W. Sung, B.Z. Tang, R. Tietze, B.N. Udugama, J.S. VanEpps, T. Weil, P.S. Weiss, I. Willner, Y. Wu, L. Yang, Z. Yue, Q. Zhang, Q. Zhang, X.-E. Zhang, Y. Zhao, X. Zhou, W.J. Parak, Diverse applications of nanomedicine, ACS Nano 11 (2017) 2313–2381, https://doi.org/10.1021/acsnano.6b06040.
[5] N. Bertrand, J. Wu, X. Xu, N. Kamaly, O.C. Farokhzad, Cancer nanotechnology: the impact of passive and active targeting in the era of modern cancer biology, Adv. Drug Deliv. Rev. 66 (2014) 2–25, https://doi.org/10.1016/j.addr.2013.11.009.
[6] R. Duivenvoorden, M.L. Senders, M.M.T. van Leent, C. Pérez-Medina, M. Nahrendorf, Z.A. Fayad, W.J.M. Mulder, Nanoimmunotherapy to treat ischaemic heart disease, Nat. Rev. Cardiol. 16 (2019) 21–32, https://doi.org/10.1038/s41569-018-0073-1.
[7] N. Benne, J. van Duijn, J. Kuiper, W. Jiskoot, B. Slütter, Orchestrating immune responses: how size, shape and rigidity affect the immunogenicity of particulate vaccines, J. Control. Release 234 (2016) 124–134, https://doi.org/10.1016/j.jconrel.2016.05.033.
[8] A. Bruinink, M. Bitar, M. Pleskova, P. Wick, H.F. Krug, K. Maniura-Weber, Addition of nanoscaled bioinspired surface features: a revolution for bone related implants and scaffolds? J. Biomed. Mater. Res. A 102 (2014) 275–294, https://doi.org/10.1002/jbm.a.34691.
[9] Z. Zhao, A. Ukidve, J. Kim, S. Mitragotri, Targeting strategies for tissue-specific drug delivery, Cell. 181 (2020) 151–167, https://doi.org/10.1016/j.cell.2020.02.001.
[10] Q. Dai, N. Bertleff-Zieschang, J.A. Braunger, M. Björnmalm, C. Cortez-Jugo, F. Caruso, Particle targeting in complex biological media, Adv. Healthc. Mater. 7 (2018), 1700575. https://doi.org/10.1002/adhm.201700575.
[11] G. Bell, Models for the specific adhesion of cells to cells, Science. 200 (1978) 618–627, https://doi.org/10.1126/science.347575.
[12] G.I. Bell, M. Dembo, P. Bongrand, Cell adhesion. Competition between nonspecific repulsion and specific bonding, Biophys. J. 45 (1984) 1051–1064, https://doi.org/10.1016/S0006-3495(84)84252-6.
[13] H. Xu, D.E. Shaw, A simple model of multivalent adhesion and its application to influenza infection, Biophys. J. 110 (2016) 218–233, https://doi.org/10.1016/j.bpj.2015.10.045.
[14] C.A. Macken, A.S. Perelson, Aggregation of cell surface receptors by multivalent ligands, J. Math. Biol. 14 (1982) 365–370, https://doi.org/10.1007/BF00275399.
[15] S. Hong, P.R. Leroueil, I.J. Majoros, B.G. Orr, J.R. Baker, M.M. Banaszak Holl, The binding avidity of a nanoparticle-based multivalent targeted drug delivery platform, Chem. Biol. 14 (2007) 107–115, https://doi.org/10.1016/j.chembiol.2006.11.015.
[16] C.B. Carlson, P. Mowery, R.M. Owen, E.C. Dykhuizen, L.L. Kiessling, Selective tumor cell targeting using low-affinity, multivalent interactions, ACS Chem. Biol. 2 (2007) 119–127, https://doi.org/10.1021/cb6003788.
[17] H. Krobath, B. Różycki, R. Lipowsky, T.R. Weikl, Binding cooperativity of membrane adhesion receptors, Soft Matter 5 (2009) 3354, https://doi.org/10.1039/b902036e.
[18] T.R. Weikl, J. Hu, G.-K. Xu, R. Lipowsky, Binding equilibrium and kinetics of membrane-anchored receptors and ligands in cell adhesion: Insights from computational model systems and theory, Cell Adhes. Migr. 10 (2016) 576–589, https://doi.org/10.1080/19336918.2016.1180487.
[19] T. Curk, J. Dobnikar, D. Frenkel, Optimal multivalent targeting of membranes with many distinct receptors, Proc. Natl. Acad. Sci. 114 (2017) 7210–7215, https://doi.org/10.1073/pnas.1704226114.
[20] O.A. Amjad, B.M. Mognetti, P. Cicuta, L. Di Michele, Membrane adhesion through bridging by multimeric ligands, Langmuir. 33 (2017) 1139–1146, https://doi.org/10.1021/acs.langmuir.6b03692.
[21] S. Angioletti-Uberti, Theory, simulations and the design of functionalized nanoparticles for biomedical applications: a soft matter perspective, Npj Comput. Mater. 3 (2017) 48, https://doi.org/10.1038/s41524-017-0050-y.
[22] M.D. Vahey, D.A. Fletcher, Influenza A virus surface proteins are organized to help penetrate host mucus, ELife. 8 (2019) e43764, https://doi.org/10.7554/eLife.43764.
[23] A.K. Pearce, R.K. O'Reilly, Insights into active targeting of nanoparticles in drug delivery: advances in clinical studies and design considerations for cancer

nanomedicine, Bioconjug. Chem. 30 (2019) 2300–2311, https://doi.org/10.1021/acs.bioconjchem.9b00456.
[24] J.W. Kim, J.R. Cochran, Targeting ligand–receptor interactions for development of cancer therapeutics, Curr. Opin. Chem. Biol. 38 (2017) 62–69, https://doi.org/10.1016/j.cbpa.2017.03.010.
[25] J. Wang, J.J. Masehi-Lano, E.J. Chung, Peptide and antibody ligands for renal targeting: nanomedicine strategies for kidney disease, Biomater. Sci. 5 (2017) 1450–1459, https://doi.org/10.1039/C7BM00271H.
[26] T. Dvir, M. Bauer, A. Schroeder, J.H. Tsui, D.G. Anderson, R. Langer, R. Liao, D.S. Kohane, Nanoparticles targeting the infarcted heart, Nano Lett. 11 (2011) 4411–4414, https://doi.org/10.1021/nl2025882.
[27] M.C. Johnston, C.J. Scott, Antibody conjugated nanoparticles as a novel form of antibody drug conjugate chemotherapy, Drug Discov. Today Technol. 30 (2018) 63–69, https://doi.org/10.1016/j.ddtec.2018.10.003.
[28] B. Sulzer, A.S. Perelson, Equilibrium binding of multivalent ligands to cells: Effects of cell and receptor density, Math. Biosci. 135 (1996) 147–185, https://doi.org/10.1016/0025-5564(96)00022-3.
[29] J. Huskens, A. Mulder, T. Auletta, C.A. Nijhuis, M.J.W. Ludden, D.N. Reinhoudt, A Model for describing the thermodynamics of multivalent host−guest interactions at interfaces, J. Am. Chem. Soc. 126 (2004) 6784–6797, https://doi.org/10.1021/ja049085k.
[30] F.J. Martinez-Veracoechea, D. Frenkel, Designing super selectivity in multivalent nano-particle binding, Proc. Natl. Acad. Sci. 108 (2011) 10963–10968, https://doi.org/10.1073/pnas.1105351108.
[31] P. Varilly, S. Angioletti-Uberti, B.M. Mognetti, D. Frenkel, A general theory of DNA-mediated and other valence-limited colloidal interactions, J. Chem. Phys. 137 (2012), 094108. https://doi.org/10.1063/1.4748100.
[32] S. Angioletti-Uberti, P. Varilly, B.M. Mognetti, A.V. Tkachenko, D. Frenkel, Communication: a simple analytical formula for the free energy of ligand–receptor-mediated interactions, J. Chem. Phys. 138 (2013), 021102. https://doi.org/10.1063/1.4775806.
[33] F.J. Martinez-Veracoechea, M.E. Leunissen, The entropic impact of tethering, multivalency and dynamic recruitment in systems with specific binding groups, Soft Matter 9 (2013) 3213, https://doi.org/10.1039/c3sm27766f.
[34] M. Mammen, S.-K. Choi, G.M. Whitesides, Polyvalent interactions in biological systems: implications for design and use of multivalent ligands and inhibitors, Angew. Chem. Int. Ed. 37 (1998) 2754–2794.
[35] W.S. Hlavacek, J.K. Percus, O.E. Percus, A.S. Perelson, C. Wofsy, Retention of antigen on follicular dendritic cells and B lymphocytes through complement-mediated multivalent ligand–receptor interactions: theory and application to HIV treatment, Math. Biosci. 176 (2002) 185–202, https://doi.org/10.1016/S0025-5564(02)00091-3.
[36] J. Vonnemann, S. Liese, C. Kuehne, K. Ludwig, J. Dernedde, C. Böttcher, R.R. Netz, R. Haag, Size dependence of steric shielding and multivalency effects for globular binding inhibitors, J. Am. Chem. Soc. 137 (2015) 2572–2579, https://doi.org/10.1021/ja5114084.
[37] S. Liese, R.R. Netz, Quantitative prediction of multivalent ligand–receptor binding affinities for influenza, cholera, and anthrax inhibition, ACS Nano 12 (2018) 4140–4147, https://doi.org/10.1021/acsnano.7b08479.
[38] D. Di Iorio, M.L. Verheijden, E. van der Vries, P. Jonkheijm, J. Huskens, Weak multivalent binding of influenza hemagglutinin nanoparticles at a sialoglycan-functionalized supported lipid bilayer, ACS Nano 13 (2019) 3413–3423, https://doi.org/10.1021/acsnano.8b09410.
[39] M. Müller, D. Lauster, H.H.K. Wildenauer, A. Herrmann, S. Block, Mobility-based quantification of multivalent virus-receptor interactions: new insights into influenza a virus binding mode, Nano Lett. 19 (2019) 1875–1882, https://doi.org/10.1021/acs.nanolett.8b04969.
[40] C.A. Mirkin, R.L. Letsinger, R.C. Mucic, A DNA-based method for rationally assembling nanoparticles into macroscopic materials, Nature. 382 (1996) 607.
[41] P.L. Biancaniello, A.J. Kim, J.C. Crocker, Colloidal interactions and self-assembly using DNA hybridization, Phys. Rev. Lett. 94 (2005), 058302. https://doi.org/10.1103/PhysRevLett.94.058302.
[42] S. Angioletti-Uberti, B.M. Mognetti, D. Frenkel, Re-entrant melting as a design principle for DNA-coated colloids, Nat. Mater. 11 (2012) 518–522, https://doi.org/10.1038/nmat3314.
[43] S. Angioletti-Uberti, P. Varilly, B.M. Mognetti, D. Frenkel, Mobile linkers on DNA-coated colloids: valency without patches, Phys. Rev. Lett. 113 (2014), 128303. https://doi.org/10.1103/PhysRevLett.113.128303.
[44] Y. Wang, Y. Wang, X. Zheng, É. Ducrot, J.S. Yodh, M. Weck, D.J. Pine, Crystallization of DNA-coated colloids, Nat. Commun. 6 (2015) 7253, https://doi.org/10.1038/ncomms8253.
[45] T. Curk, U. Bren, J. Dobnikar, Bonding interactions between ligand-decorated colloidal particles, Mol. Phys. 116 (2018) 3392–3400, https://doi.org/10.1080/00268976.2018.1503354.
[46] S.J. Bachmann, J. Kotar, L. Parolini, A. Šarić, P. Cicuta, L. Di Michele, B.M. Mognetti, Melting transition in lipid vesicles functionalised by mobile DNA linkers, Soft Matter 12 (2016) 7804–7817, https://doi.org/10.1039/C6SM01515H.
[47] B.D. Myers, Q.-Y. Lin, H. Wu, E. Luijten, C.A. Mirkin, V.P. Dravid, Size-selective nanoparticle assembly on substrates by DNA density patterning, ACS Nano 10 (2016) 5679–5686, https://doi.org/10.1021/acsnano.6b02246.
[48] S.A.J. van der Meulen, G. Helms, M. Dogterom, Solid colloids with surface-mobile linkers, J. Phys. Condens. Matter 27 (2015), 233101. https://doi.org/10.1088/0953-8984/27/23/233101.
[49] S. Angioletti-Uberti, B.M. Mognetti, D. Frenkel, Theory and simulation of DNA-coated colloids: a guide for rational design, Phys. Chem. Chem. Phys. 18 (2016) 6373–6393, https://doi.org/10.1039/C5CP06981E.
[50] Y. Zhang, A. McMullen, L.-L. Pontani, X. He, R. Sha, N.C. Seeman, J. Brujic, P.M. Chaikin, Sequential self-assembly of DNA functionalized droplets, Nat. Commun. 8 (2017) 21, https://doi.org/10.1038/s41467-017-00070-0.
[51] N.B. Tito, D. Frenkel, Switch-like surface binding of competing multivalent particles, Eur. Phys. J. Spec. Top. 225 (2016) 1673–1682, https://doi.org/10.1140/epjst/e2016-60119-6.
[52] N.B. Tito, Multivalent “attacker & guard” strategy for targeting surfaces with low receptor density, J. Chem. Phys. 150 (2019), 184907. https://doi.org/10.1063/1.5086277.
[53] X. Tian, S. Angioletti-Uberti, G. Battaglia, On the design of precision nanomedicines, Sci. Adv. 6 (2020).
[54] K.C. Tjandra, P. Thordarson, Multivalency in drug delivery–when is it too much of a good thing? Bioconjug. Chem. 30 (2019) 503–514, https://doi.org/10.1021/acs.bioconjchem.8b00804.
[55] J.-C. Leroux, Drug Delivery: Too Much Complexity, Not Enough Reproducibility? Angew. Chem. Int. Ed. 56 (2017) 15170–15171, https://doi.org/10.1002/anie.201709002.
[56] S. Wilhelm, A.J. Tavares, Q. Dai, S. Ohta, J. Audet, H.F. Dvorak, W.C.W. Chan, Analysis of nanoparticle delivery to tumours, Nat. Rev. Mater. 1 (2016) https://doi.org/10.1038/natrevmats.2016.14.
[57] K. Park, The drug delivery field at the inflection point: time to fight its way out of the egg, J. Control. Release 267 (2017) 2–14, https://doi.org/10.1016/j.jconrel.2017.07.030.
[58] D.J.A. Crommelin, P. van Hoogevest, G. Storm, The role of liposomes in clinical nanomedicine development. What now? Now what? J. Control. Release 318 (2020) 256–263, https://doi.org/10.1016/j.jconrel.2019.12.023.
[59] Q. Dai, S. Wilhelm, D. Ding, A.M. Syed, S. Sindhwani, Y. Zhang, Y.Y. Chen, P. MacMillan, W.C.W. Chan, Quantifying the ligand-coated nanoparticle delivery to cancer cells in solid tumors, ACS Nano (2018) https://doi.org/10.1021/acsnano.8b03900.
[60] E. Polo, V. Castagnola, K.A. Dawson, Understanding and characterizing functional properties of nanoparticles, Pharm. Nanotechnol. Innov. Prod., Wiley-VCH Verlag GmbH & Co. KGaA, Weinheim, Germany 2016, pp. 63–80, https://doi.org/10.1002/9783527800681.ch4.
[61] A. Beck, L. Goetsch, C. Dumontet, N. Corvaïa, Strategies and challenges for the next generation of antibody–drug conjugates, Nat. Rev. Drug Discov. 16 (2017) 315–337, https://doi.org/10.1038/nrd.2016.268.
[62] B.-Q. Shen, K. Xu, L. Liu, H. Raab, S. Bhakta, M. Kenrick, K.L. Parsons-Reponte, J. Tien, S.-F. Yu, E. Mai, D. Li, J. Tibbitts, J. Baudys, O.M. Saad, S.J. Scales, P.J. McDonald, P.E. Hass, C. Eigenbrot, T. Nguyen, W.A. Solis, R.N. Fuji, K.M. Flagella, D. Patel, S.D. Spencer, L.A. Khawli, A. Ebens, W.L. Wong, R. Vandlen, S. Kaur, M.X. Sliwkowski, R.H. Scheller, P. Polakis, J.R. Junutula, Conjugation site modulates the in vivo stability and therapeutic activity of antibody-drug conjugates, Nat. Biotechnol. 30 (2012) 184–189, https://doi.org/10.1038/nbt.2108.
[63] M. Ferrari, Frontiers in cancer nanomedicine: directing mass transport through biological barriers, Trends Biotechnol. 28 (2010) 181–188, https://doi.org/10.1016/j.tibtech.2009.12.007.
[64] E. Blanco, H. Shen, M. Ferrari, Principles of nanoparticle design for overcoming biological barriers to drug delivery, Nat. Biotechnol. 33 (2015) 941–951, https://doi.org/10.1038/nbt.3330.
[65] J. Shi, P.W. Kantoff, R. Wooster, O.C. Farokhzad, Cancer nanomedicine: progress, challenges and opportunities, Nat. Rev. Cancer 17 (2017) 20–37, https://doi.org/10.1038/nrc.2016.108.
[66] S. Tenzer, D. Docter, J. Kuharev, A. Musyanovych, V. Fetz, R. Hecht, F. Schlenk, D. Fischer, K. Kiouptsi, C. Reinhardt, K. Landfester, H. Schild, M. Maskos, S.K. Knauer, R.H. Stauber, Rapid formation of plasma protein corona critically affects nanoparticle pathophysiology, Nat. Nanotechnol. 8 (2013) 772–781, https://doi.org/10.1038/nnano.2013.181.
[67] G. Caracciolo, O.C. Farokhzad, M. Mahmoudi, Biological Identity of nanoparticles in vivo : clinical implications of the protein corona, Trends Biotechnol. 35 (2017) 257–264, https://doi.org/10.1016/j.tibtech.2016.08.011.
[68] M.P. Monopoli, C. Åberg, A. Salvati, K.A. Dawson, Biomolecular coronas provide the biological identity of nanosized materials, Nat. Nanotechnol. 7 (2012) 779–786, https://doi.org/10.1038/nnano.2012.207.
[69] A. Salvati, A.S. Pitek, M.P. Monopoli, K. Prapainop, F.B. Bombelli, D.R. Hristov, P.M. Kelly, C. Åberg, E. Mahon, K.A. Dawson, Transferrin-functionalized nanoparticles lose their targeting capabilities when a biomolecule corona adsorbs on the surface, Nat. Nanotechnol. 8 (2013) 137–143, https://doi.org/10.1038/nnano.2012.237.
[70] W. Xiao, H. Gao, The impact of protein corona on the behavior and targeting capability of nanoparticle-based delivery system, Int. J. Pharm. 552 (2018) 328–339, https://doi.org/10.1016/j.ijpharm.2018.10.011.
[71] A.K. Barui, J.Y. Oh, B. Jana, C. Kim, J. Ryu, Cancer-targeted nanomedicine: overcoming the barrier of the protein corona, Adv. Ther. 3 (2020) 1900124, https://doi.org/10.1002/adtp.201900124.
[72] E. Polo, M. Collado, B. Pelaz, P. del Pino, Advances toward more efficient targeted delivery of nanoparticles in vivo: understanding interactions between nanoparticles and cells, ACS Nano 11 (2017) 2397–2402, https://doi.org/10.1021/acsnano.7b01197.
[73] M. Howard, B.J. Zern, A.C. Anselmo, V.V. Shuvaev, S. Mitragotri, V. Muzykantov, Vascular targeting of nanocarriers: perplexing aspects of the seemingly straightforward paradigm, ACS Nano 8 (2014) 4100–4132, https://doi.org/10.1021/nn500136z.
[74] X. Tian, D.M. Leite, E. Scarpa, S. Nyberg, G. Fullstone, J. Forth, D.L. Matias, A. Apriceno, A. Poma, A. Duro-Castano, M. Vuyyuru, L. Harker-Kirschneck, A. Šarić, Z. Zhang, P. Xiang, B. Fang, Y. Tian, L. Luo, L. Rizzello, G. Battaglia, On the shuttling

across the blood-brain barrier via tubules formation: mechanism and cargo avidity bias, BioRxiv, 2020https://doi.org/10.1101/2020.04.04.025866.
[75] C. Saraiva, C. Praça, R. Ferreira, T. Santos, L. Ferreira, L. Bernardino, Nanoparticle-mediated brain drug delivery: overcoming blood–brain barrier to treat neurodegenerative diseases, J. Control. Release 235 (2016) 34–47, https://doi.org/10.1016/j.jconrel.2016.05.044.
[76] P.A. Netti, D.A. Berk, M.A. Swartz, A.J. Grodzinsky, R.K. Jain, Role of extracellular matrix assembly in interstitial transport in solid tumors, Cancer Res. 60 (2000) 2497–2503.
[77] A.B. Engin, D. Nikitovic, M. Neagu, P. Henrich-Noack, A.O. Docea, M.I. Shtilman, K. Golokhvast, A.M. Tsatsakis, Mechanistic understanding of nanoparticles' interactions with extracellular matrix: the cell and immune system, Part. Fibre Toxicol. 14 (2017) 22, https://doi.org/10.1186/s12989-017-0199-z.
[78] L.A. Lane, Physics in nanomedicine: Phenomena governing the in vivo performance of nanoparticles, Appl. Phys. Rev. 7 (2020), 011316. https://doi.org/10.1063/1.5052455.
[79] T.J. Anchordoquy, Y. Barenholz, D. Boraschi, M. Chorny, P. Decuzzi, M.A. Dobrovolskaia, Z.S. Farhangrazi, D. Farrell, A. Gabizon, H. Ghandehari, B. Godin, N.M. La-Beck, J. Ljubimova, S.M. Moghimi, L. Pagliaro, J.-H. Park, D. Peer, E. Ruoslahti, N.J. Serkova, D. Simberg, Mechanisms and barriers in cancer nanomedicine: addressing challenges, looking for solutions, ACS Nano 11 (2017) 12–18, https://doi.org/10.1021/acsnano.6b08244.
[80] Z. Cheng, A. Al Zaki, J.Z. Hui, V.R. Muzykantov, A. Tsourkas, Multifunctional nanoparticles: cost versus benefit of adding targeting and imaging capabilities, Science. 338 (2012) 903–910, https://doi.org/10.1126/science.1226338.
[81] J. Seoane, L. De Mattos-Arruda, The challenge of intratumour heterogeneity in precision medicine, J. Intern. Med. 276 (2014) 41–51, https://doi.org/10.1111/joim.12240.
[82] Y.H. Bae, K. Park, Targeted drug delivery to tumors: myths, reality and possibility, J. Control. Release 153 (2011) 198–205, https://doi.org/10.1016/j.jconrel.2011.06.001.
[83] P.L. Bedard, A.R. Hansen, M.J. Ratain, L.L. Siu, Tumour heterogeneity in the clinic, Nature. 501 (2013) 355–364, https://doi.org/10.1038/nature12627.
[84] J.-M. Rabanel, V. Adibnia, S.F. Tehrani, S. Sanche, P. Hildgen, X. Banquy, C. Ramassamy, Nanoparticle heterogeneity: an emerging structural parameter influencing particle fate in biological media? Nanoscale. 11 (2019) 383–406, https://doi.org/10.1039/C8NR04916E.
[85] N. Feiner-Gracia, M. Beck, S. Pujals, S. Tosi, T. Mandal, C. Buske, M. Linden, L. Albertazzi, Super-resolution microscopy unveils dynamic heterogeneities in nanoparticle protein corona, Small. 13 (2017), 1701631. https://doi.org/10.1002/smll.201701631.
[86] N. Feiner-Gracia, R.A. Olea, R. Fitzner, N. El Boujnouni, A.H. van Asbeck, R. Brock, L. Albertazzi, Super-resolution imaging of structure, molecular composition, and stability of single oligonucleotide polyplexes, Nano Lett. 19 (2019) 2784–2792, https://doi.org/10.1021/acs.nanolett.8b04407.
[87] D.G. Mullen, M. Fang, A. Desai, J.R. Baker, B.G. Orr, M.M. Banaszak Holl, A quantitative assessment of nanoparticle−ligand distributions: implications for targeted drug and imaging delivery in dendrimer conjugates, ACS Nano 4 (2010) 657–670, https://doi.org/10.1021/nn900999c.
[88] S.T. Johnston, M. Faria, E.J. Crampin, An analytical approach for quantifying the influence of nanoparticle polydispersity on cellular delivered dose, J. R. Soc. Interface 15 (2018), 20180364. https://doi.org/10.1098/rsif.2018.0364.
[89] C. Rodriguez-Quijada, M. Sánchez-Purrà, H. de Puig, K. Hamad-Schifferli, Physical properties of biomolecules at the nanomaterial interface, J. Phys. Chem. B 122 (2018) 2827–2840, https://doi.org/10.1021/acs.jpcb.8b00168.
[90] D. Rosenblum, N. Joshi, W. Tao, J.M. Karp, D. Peer, Progress and challenges towards targeted delivery of cancer therapeutics, Nat. Commun. 9 (2018) 1410, https://doi.org/10.1038/s41467-018-03705-y.
[91] H. Chen, W. Zhang, G. Zhu, J. Xie, X. Chen, Rethinking cancer nanotheranostics, Nat. Rev. Mater. 2 (2017) 17024, https://doi.org/10.1038/natrevmats.2017.24.
[92] A.H.-W. Yang, R.T.A. Macgillivray, J. Chen, Y. Luo, Y. Wang, G.D. Brayer, A.B. Mason, R.C. Woodworth, M.E.P. Murphy, Crystal structures of two mutants (K206Q, H207E) of the N-lobe of human transferrin with increased affinity for iron, Protein Sci. 9 (2008) 49–52, https://doi.org/10.1110/ps.9.1.49.
[93] M. Faria, M. Björnmalm, K.J. Thurecht, S.J. Kent, R.G. Parton, M. Kavallaris, A.P.R. Johnston, J.J. Gooding, S.R. Corrie, B.J. Boyd, P. Thordarson, A.K. Whittaker, M.M. Stevens, C.A. Prestidge, C.J.H. Porter, W.J. Parak, T.P. Davis, E.J. Crampin, F. Caruso, Minimum information reporting in bio–nano experimental literature, Nat. Nanotechnol. 13 (2018) 777–785, https://doi.org/10.1038/s41565-018-0246-4.
[94] J.-B. Coty, C. Vauthier, Characterization of nanomedicines: a reflection on a field under construction needed for clinical translation success, J. Control. Release 275 (2018) 254–268, https://doi.org/10.1016/j.jconrel.2018.02.013.
[95] A.M. Alkilany, L. Zhu, H. Weller, A. Mews, W.J. Parak, M. Barz, N. Feliu, Ligand density on nanoparticles: A parameter with critical impact on nanomedicine, Adv. Drug Deliv. Rev. 143 (2019) 22–36, https://doi.org/10.1016/j.addr.2019.05.010.
[96] A.A. Khorasani, J. Weaver, C. Salvador Morales, Closing the gap: accelerating the translational process in nanomedicine by proposing standardized characterization techniques, Int. J. Nanomedicine (2014) 5729, https://doi.org/10.2147/IJN.S72479.
[97] T. Curk, J. Dobnikar, D. Frenkel, Design principles for super selectivity using multivalent interactions, in: J. Huskens, L.J. Prins, R. Haag, B.J. Ravoo (Eds.), Multivalency, John Wiley & Sons, Ltd, Chichester, UK 2017, pp. 75–101, https://doi.org/10.1002/9781119143505.ch3.
[98] A.C. Newton, J. Groenewold, W.K. Kegel, P.G. Bolhuis, Rotational diffusion affects the dynamical self-assembly pathways of patchy particles, Proc. Natl. Acad. Sci. 112 (2015) 15308–15313, https://doi.org/10.1073/pnas.1513210112.
[99] A.C. Newton, J. Groenewold, W.K. Kegel, P.G. Bolhuis, The role of multivalency in the association kinetics of patchy particle complexes, J. Chem. Phys. 146 (2017), 234901. https://doi.org/10.1063/1.4984966.
[100] R. Lanfranco, P.K. Jana, L. Tunesi, P. Cicuta, B.M. Mognetti, L. Di Michele, G. Bruylants, Kinetics of nanoparticle–membrane adhesion mediated by multivalent interactions, Langmuir. 35 (2019) 2002–2012, https://doi.org/10.1021/acs.langmuir.8b02707.
[101] S. Block, V.P. Zhdanov, F. Höök, Quantification of multivalent interactions by tracking single biological nanoparticle mobility on a lipid membrane, Nano Lett. 16 (2016) 4382–4390, https://doi.org/10.1021/acs.nanolett.6b01511.
[102] S. Jan Bachmann, M. Petitzon, B.M. Mognetti, Bond formation kinetics affects self-assembly directed by ligand–receptor interactions, Soft Matter 12 (2016) 9585–9592, https://doi.org/10.1039/C6SM02016J.
[103] A. Vijaykumar, P.R. ten Wolde, P.G. Bolhuis, Generalised expressions for the association and dissociation rate constants of molecules with multiple binding sites, Mol. Phys. 116 (2018) 3042–3054, https://doi.org/10.1080/00268976.2018.1473653.
[104] N.A. Licata, A.V. Tkachenko, Kinetic limitations of cooperativity-based drug delivery systems, Phys. Rev. Lett. 100 (2008), 158102. https://doi.org/10.1103/PhysRevLett.100.158102.
[105] J. Lin, K. Wang, X. Xia, L. Shen, Quantification of multivalency in protein-oligomer-coated nanoparticles targeting dynamic membrane glycan receptors, Langmuir. 34 (2018) 8415–8421.
[106] X. Montet, M. Funovics, K. Montet-Abou, R. Weissleder, L. Josephson, Multivalent effects of RGD peptides obtained by nanoparticle display, J. Med. Chem. 49 (2006) 6087–6093, https://doi.org/10.1021/jm060515m.
[107] C.M. Csizmar, J.R. Petersburg, T.J. Perry, L. Rozumalski, B.J. Hackel, C.R. Wagner, Multivalent ligand binding to cell membrane antigens: defining the interplay of affinity, valency, and expression density, J. Am. Chem. Soc. 141 (2019) 251–261, https://doi.org/10.1021/jacs.8b09198.
[108] G.V. Dubacheva, T. Curk, D. Frenkel, R.P. Richter, Multivalent recognition at fluid surfaces: the interplay of receptor clustering and superselectivity, J. Am. Chem. Soc. 141 (2019) 2577–2588, https://doi.org/10.1021/jacs.8b12553.
[109] D. Di Iorio, Y. Lu, J. Meulman, J. Huskens, Recruitment of receptors at supported lipid bilayers promoted by the multivalent binding of ligand-modified unilamellar vesicles, Chem. Sci. 11 (2020) 3307–3315, https://doi.org/10.1039/D0SC00518E.
[110] G.V. Dubacheva, T. Curk, B.M. Mognetti, R. Auzély-Velty, D. Frenkel, R.P. Richter, Superselective targeting using multivalent polymers, J. Am. Chem. Soc. 136 (2014) 1722–1725, https://doi.org/10.1021/ja411138s.
[111] R. Hammink, S. Mandal, L.J. Eggermont, M. Nooteboom, Controlling T-cell activation with synthetic dendritic cells using the multivalency effect, ACS Omega. (2017) 10.
[112] S. Wang, E.E. Dormidontova, Selectivity of ligand-receptor interactions between nanoparticle and cell surfaces, Phys. Rev. Lett. 109 (2012), 238102. https://doi.org/10.1103/PhysRevLett.109.238102.
[113] T. Curk, N.B. Tito, First-order 'hyper-selective' binding transition of multivalent particles under force, J. Phys. Condens. Matter 32 (2020), 214002. https://doi.org/10.1088/1361-648X/ab6d12.
[114] J. Lowensohn, B. Oyarzún, G. Narváez Paliza, B.M. Mognetti, W.B. Rogers, Linker-mediated phase behavior of DNA-coated colloids, Phys. Rev. X. 9 (2019), 041054. https://doi.org/10.1103/PhysRevX.9.041054.
[115] P.K. Jana, B.M. Mognetti, Surface-triggered cascade reactions between DNA linkers direct the self-assembly of colloidal crystals of controllable thickness, Nanoscale. 11 (2019) 5450–5459, https://doi.org/10.1039/C8NR10217A.
[116] A. Ahmed, Myocardial beta-1 adrenoceptor down-regulation in aging and heart failure: implications for beta-blocker use in older adults with heart failure, Eur. J. Heart Fail. 5 (2003) 709–715, https://doi.org/10.1016/S1388-9842(03)00058-8.
[117] P. Seeman, H.B. Niznik, Dopamine receptors and transporters in Parkinson's disease and schizophrenia, FASEB J. 4 (1990) 2737–2744, https://doi.org/10.1096/fasebj.4.10.2197154.
[118] M.F. Rimawi, R. Schiff, C.K. Osborne, Targeting HER2 for the treatment of breast cancer, Annu. Rev. Med. 66 (2015) 111–128, https://doi.org/10.1146/annurev-med-042513-015127.
[119] N. Iqbal, N. Iqbal, Human epidermal growth factor receptor 2 (HER2) in cancers: overexpression and therapeutic implications, Mol. Biol. Int. 2014 (2014) 1–9, https://doi.org/10.1155/2014/852748.
[120] J. Wang, B. Xu, Targeted therapeutic options and future perspectives for HER2-positive breast cancer, Signal Transduct. Target. Ther. 4 (2019) 34, https://doi.org/10.1038/s41392-019-0069-2.
[121] M. Colombo, F. Corsi, D. Foschi, E. Mazzantini, S. Mazzucchelli, C. Morasso, E. Occhipinti, L. Polito, D. Prosperi, S. Ronchi, P. Verderio, HER2 targeting as a two-sided strategy for breast cancer diagnosis and treatment: Outlook and recent implications in nanomedical approaches, Pharmacol. Res. 62 (2010) 150–165, https://doi.org/10.1016/j.phrs.2010.01.013.
[122] V.G. Abramson, I.A. Mayer, Molecular heterogeneity of triple-negative breast cancer, Curr. Breast Cancer Rep. 6 (2014) 154–158, https://doi.org/10.1007/s12609-014-0152-1.
[123] J.T. Duskey, K.G. Rice, Nanoparticle ligand presentation for targeting solid tumors, AAPS PharmSciTech 15 (2014) 1345–1354, https://doi.org/10.1208/s12249-014-0143-6.
[124] L. Bareford, P. Swaan, Endocytic mechanisms for targeted drug delivery, Adv. Drug Deliv. Rev. 59 (2007) 748–758, https://doi.org/10.1016/j.addr.2007.06.008.
[125] Y. Yarden, G. Pines, The ERBB network: at last, cancer therapy meets systems biology, Nat. Rev. Cancer 12 (2012) 553–563, https://doi.org/10.1038/nrc3309.
[126] D. Rozbesky, E.Y. Jones, Cell guidance ligands, receptors and complexes – orchestrating signalling in time and space, Curr. Opin. Struct. Biol. 61 (2020) 79–85, https://doi.org/10.1016/j.sbi.2019.11.007.

[127] G. Gocheva, A. Ivanova, A look at receptor–ligand pairs for active-targeting drug delivery from crystallographic and molecular dynamics perspectives, Mol. Pharm. 16 (2019) 3293–3321, https://doi.org/10.1021/acs.molpharmaceut.9b00250.
[128] A. Pandit, L. Khare, P.V. Devarajan, R. Jain, P. Dandekar, Breast cancer receptors and targeting strategies, in: P.V. Devarajan, P. Dandekar, A.A. D'Souza (Eds.), Target. Intracell. Drug Deliv. Recept. Mediat. Endocytosis, Springer International Publishing, Cham 2019, pp. 79–108, https://doi.org/10.1007/978-3-030-29168-6_3.
[129] J.I. Hare, T. Lammers, M.B. Ashford, S. Puri, G. Storm, S.T. Barry, Challenges and strategies in anti-cancer nanomedicine development: an industry perspective, Adv. Drug Deliv. Rev. 108 (2017) 25–38, https://doi.org/10.1016/j.addr.2016.04.025.
[130] G. Turashvili, E. Brogi, Tumor Heterogeneity in Breast Cancer, Front. Med. 4 (2017) 227, https://doi.org/10.3389/fmed.2017.00227.
[131] D.L. Dexter, P. Calabresi, Intraneoplastic diversity, Biochim. Biophys. Acta BBA - Rev. Cancer. 695 (1982) 97–112, https://doi.org/10.1016/0304-419X(82)90019-1.
[132] G.H. Heppner, B.E. Miller, Tumor heterogeneity: biological implications and therapeutic consequences, Cancer Metastasis Rev. 2 (1983) 5–23, https://doi.org/10.1007/BF00046903.
[133] I.J. Fidler, M.L. Kripke, The challenge of targeting metastasis, Cancer Metastasis Rev. 34 (2015) 635–641, https://doi.org/10.1007/s10555-015-9586-9.
[134] J. Gao, Y. Wang, M. Cai, Y. Pan, H. Xu, J. Jiang, H. Ji, H. Wang, Mechanistic insights into EGFR membrane clustering revealed by super-resolution imaging, Nanoscale. 7 (2015) 2511–2519, https://doi.org/10.1039/C4NR04962D.
[135] M. Boggara, K. Athmakuri, S. Srivastava, R. Cole, R.S. Kane, Characterization of the diffusion of epidermal growth factor receptor clusters by single particle tracking, Biochim. Biophys. Acta Biomembr. 1828 (2013) 419–426, https://doi.org/10.1016/j.bbamem.2012.08.022.
[136] M.S. Brown, R.G.W. Anderson, J.L. Goldstein, Recycling receptors: the round-trip itinerary of migrant membrane proteins, Cell. 32 (1983) 663–667, https://doi.org/10.1016/0092-8674(83)90052-1.
[137] F.R. Maxfield, T.E. McGraw, Endocytic recycling, Nat. Rev. Mol. Cell Biol. 5 (2004) 121–132, https://doi.org/10.1038/nrm1315.
[138] S. Maramotti, M. Paci, G. Manzotti, C. Rapicetta, M. Gugnoni, C. Galeone, A. Cesario, F. Lococo, Soluble epidermal growth factor receptors (sEGFRs) in cancer: biological aspects and clinical relevance, Int. J. Mol. Sci. 17 (2016) 593, https://doi.org/10.3390/ijms17040593.
[139] S.-H. Tseng, M.-Y. Chou, I.-M. Chu, Cetuximab-conjugated iron oxide nanoparticles for cancer imaging and therapy, Int. J. Nanomedicine (2015) 3663, https://doi.org/10.2147/IJN.S80134.
[140] G.T. Tietjen, W.M. Saltzman, Nanomedicine gets personal, Sci. Transl. Med. 7 (2015) https://doi.org/10.1126/scitranslmed.aad6645314fs47-314fs47.
[141] T. Lammers, L.Y. Rizzo, G. Storm, F. Kiessling, Personalized Nanomedicine, Clin. Cancer Res. 18 (2012) 4889–4894, https://doi.org/10.1158/1078-0432.CCR-12-1414.
[142] I.S. Vizirianakis, D.G. Fatouros, Personalized nanomedicine: paving the way to the practical clinical utility of genomics and nanotechnology advancements, Adv. Drug Deliv. Rev. 64 (2012) 1359–1362, https://doi.org/10.1016/j.addr.2012.09.034.
[143] C. Fornaguera, M. García-Celma, Personalized nanomedicine: a revolution at the nanoscale, J. Pers. Med. 7 (2017) 12, https://doi.org/10.3390/jpm7040012.
[144] J. Lazarovits, Y.Y. Chen, F. Song, W. Ngo, A.J. Tavares, Y.-N. Zhang, J. Audet, B. Tang, Q. Lin, M.C. Tleugabulova, S. Wilhelm, J.R. Krieger, T. Mallevaey, W.C.W. Chan, Synthesis of patient-specific nanomaterials, Nano Lett. 19 (2019) 116–123, https://doi.org/10.1021/acs.nanolett.8b03434.
[145] H.J. Han, C. Ekweremadu, N. Patel, Advanced drug delivery system with nanomaterials for personalised medicine to treat breast cancer, J. Drug Deliv. Sci. Technol. 52 (2019) 1051–1060, https://doi.org/10.1016/j.jddst.2019.05.024.
[146] A. Kaushik, R.D. Jayant, V. Bhardwaj, M. Nair, Personalized nanomedicine for CNS diseases, Drug Discov. Today 23 (2018) 1007–1015, https://doi.org/10.1016/j.drudis.2017.11.010.
[147] K.M. Tichauer, Y. Wang, B.W. Pogue, J.T.C. Liu, Quantitative in vivo cell-surface receptor imaging in oncology: kinetic modeling and paired-agent principles from nuclear medicine and optical imaging, Phys. Med. Biol. 60 (2015) R239–R269, https://doi.org/10.1088/0031-9155/60/14/R239.
[148] Caprio Salvatore, Sarnella Hill, Zannetti Roviello, Recent advances in nuclear imaging of receptor expression to guide targeted therapies in breast cancer, Cancers. 11 (2019) 1614, https://doi.org/10.3390/cancers11101614.
[149] R.L. Camp, M. Dolled-Filhart, B.L. King, D.L. Rimm, Quantitative analysis of breast cancer tissue microarrays shows that both high and normal levels of HER2 expression are associated with poor outcome, Cancer Res. 63 (2003) 1445–1448.
[150] R.L. Camp, G.G. Chung, D.L. Rimm, Automated subcellular localization and quantification of protein expression in tissue microarrays, Nat. Med. 8 (2002) 1323–1328, https://doi.org/10.1038/nm791.
[151] D. Faratian, J. Christiansen, M. Gustavson, C. Jones, C. Scott, I. Um, D.J. Harrison, Heterogeneity mapping of protein expression in tumors using quantitative immunofluorescence, J. Vis. Exp. (2011) 3334, https://doi.org/10.3791/3334.
[152] M.D. Onsum, E. Geretti, V. Paragas, A.J. Kudla, S.P. Moulis, L. Luus, T.J. Wickham, C.F. McDonagh, G. MacBeath, B.S. Hendriks, Single-cell quantitative HER2 measurement identifies heterogeneity and distinct subgroups within traditionally defined HER2-positive patients, Am. J. Pathol. 183 (2013) 1446–1460, https://doi.org/10.1016/j.ajpath.2013.07.015.
[153] W. Wang, Y. Yang, S. Wang, V.J. Nagaraj, Q. Liu, J. Wu, N. Tao, Label-free measuring and mapping of binding kinetics of membrane proteins in single living cells, Nat. Chem. 4 (2012) 846–853, https://doi.org/10.1038/nchem.1434.
[154] W. Wang, L. Yin, L. Gonzalez-Malerva, S. Wang, X. Yu, S. Eaton, S. Zhang, H.-Y. Chen, J. LaBaer, N. Tao, In situ drug-receptor binding kinetics in single cells: a quantitative label-free study of anti-tumor drug resistance, Sci. Rep. 4 (2015) 6609, https://doi.org/10.1038/srep06609.
[155] F. Zhang, S. Wang, L. Yin, Y. Yang, Y. Guan, W. Wang, H. Xu, N. Tao, Quantification of epidermal growth factor receptor expression level and binding kinetics on cell surfaces by surface plasmon resonance imaging, Anal. Chem. 87 (2015) 9960–9965, https://doi.org/10.1021/acs.analchem.5b02572.
[156] R. Ramji, C.F. Cheong, H. Hirata, A.R.A. Rahman, C.T. Lim, Rapid quantification of live cell receptors using bioluminescence in a flow-based microfluidic device, Small. 11 (2015) 943–951, https://doi.org/10.1002/smll.201401674.
[158] C.F. Cahall, J.L. Lilly, E.A. Hirschowitz, B.J. Berron, A quantitative perspective on surface marker selection for the isolation of functional tumor cells, Breast Cancer Basic Clin. Res. (2015) https://doi.org/10.4137/BCBCR.S25461.
[159] P.I. Imoukhuede, A.S. Popel, Quantification and cell-to-cell variation of vascular endothelial growth factor receptors, Exp. Cell Res. 317 (2011) 955–965, https://doi.org/10.1016/j.yexcr.2010.12.014.
[160] J. Wang, J. Min, S.A. Eghtesadi, R.S. Kane, A. Chilkoti, Quantitative study of the interaction of multivalent ligand-modified nanoparticles with breast cancer cells with tunable receptor density, ACS Nano 14 (2020) 372–383, https://doi.org/10.1021/acsnano.9b05689.
[161] S. Chen, P.I. Imoukhuede, Single-cell receptor quantification of an in vitro coculture angiogenesis model reveals VEGFR, NRP1, Tie2, and PDGFR regulation and endothelial heterogeneity, Processes. 7 (2019) 356, https://doi.org/10.3390/pr7060356.
[162] J. Vangindertael, R. Camacho, W. Sempels, H. Mizuno, P. Dedecker, K.P.F. Janssen, An introduction to optical super-resolution microscopy for the adventurous biologist, Methods Appl. Fluoresc. 6 (2018), 022003. https://doi.org/10.1088/2050-6120/aaae0c.
[163] K.S. Gruβmayer, K. Yserentant, D.-P. Herten, Photons in - numbers out: perspectives in quantitative fluorescence microscopy for in situ protein counting, Methods Appl. Fluoresc. 7 (2019), 012003. https://doi.org/10.1088/2050-6120/aaf2eb.
[164] M.S. Dietz, M. Heilemann, Optical super-resolution microscopy unravels the molecular composition of functional protein complexes, Nanoscale. 11 (2019) 17981–17991, https://doi.org/10.1039/C9NR06364A.
[165] S.J. Tobin, D.L. Wakefield, V. Jones, X. Liu, D. Schmolze, T. Jovanović-Talisman, Single molecule localization microscopy coupled with touch preparation for the quantification of trastuzumab-bound HER2, Sci. Rep. 8 (2018) https://doi.org/10.1038/s41598-018-33225-0.
[166] M.A. Gomes de Castro, H. Wildhagen, S. Sograte-Idrissi, C. Hitzing, M. Binder, M. Trepel, N. Engels, F. Opazo, Differential organization of tonic and chronic B cell antigen receptors in the plasma membrane, Nat. Commun. 10 (2019) 820, https://doi.org/10.1038/s41467-019-08677-1.
[167] A. Conway, T. Vazin, D.P. Spelke, N.A. Rode, K.E. Healy, R.S. Kane, D.V. Schaffer, Multivalent ligands control stem cell behaviour in vitro and in vivo, Nat. Nanotechnol. 8 (2013) 831–838, https://doi.org/10.1038/nnano.2013.205.
[168] A. Ianoul, M. Street, D. Grant, J. Pezacki, R.S. Taylor, L.J. Johnston, Near-field scanning fluorescence microscopy study of ion channel clusters in cardiac myocyte membranes, Biophys. J. 87 (2004) 3525–3535, https://doi.org/10.1529/biophysj.104.046383.
[169] A. Ianoul, D.D. Grant, Y. Rouleau, M. Bani-Yaghoub, L.J. Johnston, J.P. Pezacki, Imaging nanometer domains of β-adrenergic receptor complexes on the surface of cardiac myocytes, Nat. Chem. Biol. 1 (2005) 196–202, https://doi.org/10.1038/nchembio726.
[170] A. Abulrob, Z. Lu, E. Baumann, D. Vobornik, R. Taylor, D. Stanimirovic, L.J. Johnston, Nanoscale imaging of epidermal growth factor receptor clustering: effects of inhibitors, J. Biol. Chem. 285 (2010) 3145–3156, https://doi.org/10.1074/jbc.M109.073338.
[171] E. Betzig, G.H. Patterson, R. Sougrat, O.W. Lindwasser, S. Olenych, J.S. Bonifacino, M.W. Davidson, J. Lippincott-Schwartz, H.F. Hess, Imaging intracellular fluorescent proteins at nanometer resolution, Science. 313 (2006) 1642–1645, https://doi.org/10.1126/science.1127344.
[172] M. Bates, B. Huang, G.T. Dempsey, X. Zhuang, Multicolor super-resolution imaging with photo-switchable fluorescent probes, Science. 317 (2007) 1749–1753, https://doi.org/10.1126/science.1146598.
[173] M. Heilemann, S. van de Linde, M. Schüttpelz, R. Kasper, B. Seefeldt, A. Mukherjee, P. Tinnefeld, M. Sauer, Subdiffraction-resolution fluorescence imaging with conventional fluorescent probes, Angew. Chem. Int. Ed. 47 (2008) 6172–6176, https://doi.org/10.1002/anie.200802376.
[174] E. Rittweger, K.Y. Han, S.E. Irvine, C. Eggeling, S.W. Hell, STED microscopy reveals crystal colour centres with nanometric resolution, Nat. Photonics 3 (2009) 144–147, https://doi.org/10.1038/nphoton.2009.2.
[175] M. Dai, R. Jungmann, P. Yin, Optical imaging of individual biomolecules in densely packed clusters, Nat. Nanotechnol. 11 (2016) 798–807, https://doi.org/10.1038/nnano.2016.95.
[176] M.B. Stone, S.A. Shelby, S.L. Veatch, Super-resolution microscopy: shedding light on the cellular plasma membrane, Chem. Rev. 117 (2017) 7457–7477, https://doi.org/10.1021/acs.chemrev.6b00716.
[177] P. Ilgen, S. Stoldt, L.-C. Conradi, C.A. Wurm, J. Rüschoff, B.M. Ghadimi, T. Liersch, S. Jakobs, STED super-resolution microscopy of clinical paraffin-embedded human rectal cancer tissue, PLoS One 9 (2014), e101563. https://doi.org/10.1371/journal.pone.0101563.
[178] H. Ta, J. Keller, M. Haltmeier, S.K. Saka, J. Schmied, F. Opazo, P. Tinnefeld, A. Munk, S.W. Hell, Mapping molecules in scanning far-field fluorescence nanoscopy, Nat. Commun. 6 (2015) 7977, https://doi.org/10.1038/ncomms8977.
[179] T. Nerreter, S. Letschert, R. Götz, S. Doose, S. Danhof, H. Einsele, M. Sauer, M. Hudecek, Super-resolution microscopy reveals ultra-low CD19 expression on myeloma cells that triggers elimination by CD19 CAR-T, Nat. Commun. 10 (2019) 3137, https://doi.org/10.1038/s41467-019-10948-w.

[180] S. Siddig, S. Aufmkolk, S. Doose, M.-L. Jobin, C. Werner, M. Sauer, D. Calebiro, Super-resolution imaging reveals the nanoscale organization of metabotropic glutamate receptors at presynaptic active zones, Sci. Adv. 6 (2020) eaay7193, https://doi.org/10.1126/sciadv.aay7193.
[181] M.S. Dietz, F. Fricke, C.L. Krüger, H.H. Niemann, M. Heilemann, Receptor-ligand interactions: binding affinities studied by single-molecule and super-resolution microscopy on intact cells, ChemPhysChem. 15 (2014) 671–676, https://doi.org/10.1002/cphc.201300755.
[182] R. Jungmann, M.S. Avendaño, M. Dai, J.B. Woehrstein, S.S. Agasti, Z. Feiger, A. Rodal, P. Yin, Quantitative super-resolution imaging with qPAINT, Nat. Methods 13 (2016) 439–442, https://doi.org/10.1038/nmeth.3804.
[183] I. Jayasinghe, A.H. Clowsley, R. Lin, T. Lutz, C. Harrison, E. Green, D. Baddeley, L. Di Michele, C. Soeller, True molecular scale visualization of variable clustering properties of ryanodine receptors, Cell Rep. 22 (2018) 557–567, https://doi.org/10.1016/j.celrep.2017.12.045.
[184] J.L. Werbin, M.S. Avendaño, V. Becker, R. Jungmann, P. Yin, G. Danuser, P.K. Sorger, Multiplexed exchange-PAINT imaging reveals ligand-dependent EGFR and Met interactions in the plasma membrane, Sci. Rep. 7 (2017) 12150, https://doi.org/10.1038/s41598-017-12257-y.
[185] M.-L.I.E. Harwardt, M.S. Schröder, Y. Li, S. Malkusch, P. Freund, S. Gupta, N. Janjic, S. Strauss, R. Jungmann, M.S. Dietz, M. Heilemann, Single-molecule super-resolution microscopy reveals heteromeric complexes of MET and EGFR upon *ligand activation*, Int. J. Mol. Sci. 21 (2020) 2803, https://doi.org/10.3390/ijms21082803.
[186] S. Pujals, N. Feiner-Gracia, L. Albertazzi, Unveiling complex structure and dynamics in supramolecular biomaterials using super-resolution microscopy, Self-Assem. Biomater, Elsevier 2018, pp. 251–274, https://doi.org/10.1016/B978-0-08-102015-9.00013-7.
[187] D.Yu. Orlova, I. Borisov, V.S. Kozhevnikov, V.P. Maltsev, A.V. Chernyshev, Distribution function approach to the study of the kinetics of IgM antibody binding to FcγRIIIb (CD16b) receptors on neutrophils by flow cytometry, J. Theor. Biol. 290 (2011) 1–6, https://doi.org/10.1016/j.jtbi.2011.08.026.
[188] M. Faria, M. Björnmalm, E.J. Crampin, F. Caruso, A few clarifications on MIRIBEL, Nat. Nanotechnol. 15 (2020) 2–3, https://doi.org/10.1038/s41565-019-0612-x.
[189] M. Srinivasarao, P.S. Low, Ligand-targeted drug delivery, Chem. Rev. 117 (2017) 12133–12164, https://doi.org/10.1021/acs.chemrev.7b00013.
[190] N.G. Welch, J.A. Scoble, B.W. Muir, P.J. Pigram, Orientation and characterization of immobilized antibodies for improved immunoassays (Review), Biointerphases. 12 (2017) 02D301, https://doi.org/10.1116/1.4978435.
[191] R.A.J. Post, D. van der Zwaag, G. Bet, S.P.W. Wijnands, L. Albertazzi, E.W. Meijer, R.W. van der Hofstad, A stochastic view on surface inhomogeneity of nanoparticles, Nat. Commun. 10 (2019) 1663, https://doi.org/10.1038/s41467-019-09595-y.
[192] D.G. Mullen, M.M. Banaszak Holl, Heterogeneous ligand–nanoparticle distributions: a major obstacle to scientific understanding and commercial translation, Acc. Chem. Res. 44 (2011) 1135–1145, https://doi.org/10.1021/ar1001389.
[193] A.J. Sivaram, A. Wardiana, C.B. Howard, S.M. Mahler, K.J. Thurecht, Recent advances in the generation of antibody-nanomaterial conjugates, Adv. Healthc. Mater. 7 (2018), 1700607. https://doi.org/10.1002/adhm.201700607.
[194] K. Tripathi, J.D. Driskell, Quantifying bound and active antibodies conjugated to gold nanoparticles: a comprehensive and robust approach to evaluate immobilization chemistry, ACS Omega. 3 (2018) 8253–8259, https://doi.org/10.1021/acsomega.8b00591.
[195] K.W. Yong, D. Yuen, M.Z. Chen, C.J.H. Porter, A.P.R. Johnston, Pointing in the right direction: controlling the orientation of proteins on nanoparticles improves targeting efficiency, Nano Lett. (2019) https://doi.org/10.1021/acs.nanolett.8b04916.
[196] A.C. Marques, P.J. Costa, S. Velho, M.H. Amaral, Functionalizing nanoparticles with cancer-targeting antibodies: a comparison of strategies, J. Control. Release 320 (2020) 180–200, https://doi.org/10.1016/j.jconrel.2020.01.035.
[197] R. Capomaccio, I. Ojea Jimenez, P. Colpo, D. Gilliland, G. Ceccone, F. Rossi, L. Calzolai, Determination of the structure and morphology of gold nanoparticle–HSA protein complexes, Nanoscale. 7 (2015) 17653–17657, https://doi.org/10.1039/C5NR05147A.
[198] N.A. Byzova, I.V. Safenkova, E.S. Slutskaya, A.V. Zherdev, B.B. Dzantiev, Less is more: a comparison of antibody–gold nanoparticle conjugates of different ratios, Bioconjug. Chem. 28 (2017) 2737–2746, https://doi.org/10.1021/acs.bioconjchem.7b00489.
[199] M. Pannuzzo, S. Esposito, L.-P. Wu, J. Key, S. Aryal, C. Celia, L. di Marzio, S.M. Moghimi, P. Decuzzi, Overcoming nanoparticle-mediated complement activation by surface PEG-pairing, Nano Lett. (2020) https://doi.org/10.1021/acs.nanolett.0c01011acs.nanolett.0c01011.
[200] J. Mosquera, I. García, M. Henriksen-Lacey, M. Martínez-Calvo, M. Dhanjani, J.L. Mascareñas, L.M. Liz-Marzán, Reversible control of protein corona formation on gold nanoparticles using host–guest interactions, ACS Nano (2020) https://doi.org/10.1021/acsnano.9b08752acsnano.9b08752.
[201] A.M. Smith, K.A. Johnston, S.E. Crawford, L.E. Marbella, J.E. Millstone, Ligand density quantification on colloidal inorganic nanoparticles, Analyst 142 (2017) 11–29, https://doi.org/10.1039/C6AN02206E.
[202] L. Martínez-Jothar, S. Doulkeridou, R.M. Schiffelers, J. Sastre Torano, S. Oliveira, C.F. van Nostrum, W.E. Hennink, Insights into maleimide-thiol conjugation chemistry: Conditions for efficient surface functionalization of nanoparticles for receptor targeting, J. Control. Release 282 (2018) 101–109, https://doi.org/10.1016/j.jconrel.2018.03.002.
[203] D. Duan, A. Wang, L. Ni, L. Zhang, X. Yan, Y. Jiang, H. Mu, Z. Wu, K. Sun, Y. Li, Trastuzumab- and Fab' fragment-modified curcumin PEG-PLGA nanoparticles: preparation and evaluation in vitro and in vivo, Int. J. Nanomedicine 13 (2018) 1831–1840, https://doi.org/10.2147/IJN.S153795.
[204] K.B. Johnsen, M. Bak, F. Melander, M.S. Thomsen, A. Burkhart, P.J. Kempen, T.L. Andresen, T. Moos, Modulating the antibody density changes the uptake and transport at the blood-brain barrier of both transferrin receptor-targeted gold nanoparticles and liposomal cargo, J. Control. Release 295 (2019) 237–249, https://doi.org/10.1016/j.jconrel.2019.01.005.
[205] L. Zhang, D. Hu, M. Salmain, B. Liedberg, S. Boujday, Direct quantification of surface coverage of antibody in IgG-Gold nanoparticles conjugates, Talanta. (2019) https://doi.org/10.1016/j.talanta.2019.05.104.
[206] J. Patel, J. Amrutiya, P. Bhatt, A. Javia, M. Jain, A. Misra, Targeted delivery of monoclonal antibody conjugated docetaxel loaded PLGA nanoparticles into EGFR overexpressed lung tumour cells, J. Microencapsul. 35 (2018) 204–217, https://doi.org/10.1080/02652048.2018.1453560.
[207] P.D. Quevedo, T. Behnke, U. Resch-Genger, Streptavidin conjugation and quantification—a method evaluation for nanoparticles, Anal. Bioanal. Chem. 408 (2016) 4133–4149, https://doi.org/10.1007/s00216-016-9510-3.
[208] R.J. Kessler, D.D. Fanestil, Interference by lipids in the determination of protein using bicinchoninic acid, Anal. Biochem. 159 (1986) 138–142, https://doi.org/10.1016/0003-2697(86)90318-0.
[209] P.M. Valencia, M.H. Hanewich-Hollatz, W. Gao, F. Karim, R. Langer, R. Karnik, O.C. Farokhzad, Effects of ligands with different water solubilities on self-assembly and properties of targeted nanoparticles, Biomaterials. 32 (2011) 6226–6233, https://doi.org/10.1016/j.biomaterials.2011.04.078.
[210] J. Ashby, Y. Duan, E. Ligans, M. Tamsi, W. Zhong, High-throughput profiling of nanoparticle–protein interactions by fluorescamine labeling, Anal. Chem. 87 (2015) 2213–2219, https://doi.org/10.1021/ac5036814.
[211] N. Graf, D.R. Bielenberg, N. Kolishetti, C. Muus, J. Banyard, O.C. Farokhzad, S.J. Lippard, αVβ3 integrin-targeted PLGA-PEG nanoparticles for enhanced anti-tumor efficacy of a Pt(IV) prodrug, ACS Nano 6 (2012) 4530–4539, https://doi.org/10.1021/nn301148e.
[212] K. Abstiens, M. Gregoritza, A.M. Goepferich, Ligand density and linker length are critical factors for multivalent nanoparticle–receptor interactions, ACS Appl. Mater. Interfaces 11 (2019) 1311–1320, https://doi.org/10.1021/acsami.8b18843.
[213] D. Bouzas-Ramos, L. Trapiella-Alfonso, K. Pons, J.R. Encinar, J.M. Costa-Fernández, V. Tsatsaris, N. Gagey-Eilstein, Controlling ligand surface density on streptavidin-magnetic particles by a simple, rapid, and reliable chemiluminescent test, Bioconjug. Chem. 29 (2018) 2646–2653, https://doi.org/10.1021/acs.bioconjchem.8b00347.
[214] M. Colombo, L. Fiandra, G. Alessio, S. Mazzucchelli, M. Nebuloni, C. De Palma, K. Kantner, B. Pelaz, R. Rotem, F. Corsi, W.J. Parak, D. Prosperi, Tumour homing and therapeutic effect of colloidal nanoparticles depend on the number of attached antibodies, Nat. Commun. 7 (2016) 13818, https://doi.org/10.1038/ncomms13818.
[215] D.G. Mullen, E.L. Borgmeier, M. Fang, D.Q. McNerny, A. Desai, J.R. Baker, B.G. Orr, M.M. Banaszak Holl, Effect of mass transport in the synthesis of partially acetylated dendrimer: implications for functional ligand−nanoparticle distributions, Macromolecules. 43 (2010) 6577–6587, https://doi.org/10.1021/ma100663c.
[216] D. Casanova, D. Giaume, M. Moreau, J.-L. Martin, T. Gacoin, J.-P. Boilot, A. Alexandrou, Counting the number of proteins coupled to single nanoparticles, J. Am. Chem. Soc. 129 (2007) 12592–12593, https://doi.org/10.1021/ja0731975.
[217] S. Dominguez-Medina, L. Kisley, L.J. Tauzin, A. Hoggard, B. Shuang, A.S.D.S. Indrasekara, S. Chen, L.-Y. Wang, P.J. Derry, A. Liopo, E.R. Zubarev, C.F. Landes, S. Link, Adsorption and unfolding of a single protein triggers nanoparticle aggregation, ACS Nano 10 (2016) 2103–2112, https://doi.org/10.1021/acsnano.5b06439.
[218] A.M. Sydor, K.J. Czymmek, E.M. Puchner, V. Mennella, Super-resolution microscopy: from single molecules to supramolecular assemblies, Trends Cell Biol. 25 (2015) 730–748, https://doi.org/10.1016/j.tcb.2015.10.004.
[219] L. Belfiore, L.M. Spenkelink, M. Ranson, A.M. van Oijen, K.L. Vine, Quantification of ligand density and stoichiometry on the surface of liposomes using single-molecule fluorescence imaging, J. Control. Release 278 (2018) 80–86, https://doi.org/10.1016/j.jconrel.2018.03.022.
[220] S. Pujals, L. Albertazzi, Super-resolution microscopy for nanomedicine research, ACS Nano 13 (2019) 9707–9712, https://doi.org/10.1021/acsnano.9b05289.
[221] S. Pujals, N. Feiner-Gracia, P. Delcanale, I. Voets, L. Albertazzi, Super-resolution microscopy as a powerful tool to study complex synthetic materials, Nat. Rev. Chem. 3 (2019) 68–84, https://doi.org/10.1038/s41570-018-0070-2.
[222] N. Mustafaoglu, T. Kiziltepe, B. Bilgicer, Site-specific conjugation of an antibody on a gold nanoparticle surface for one-step diagnosis of prostate specific antigen with dynamic light scattering, Nanoscale. 9 (2017) 8684–8694, https://doi.org/10.1039/C7NR03096G.
[223] C. Parolo, A. de la Escosura-Muñiz, E. Polo, V. Grazú, J.M. de la Fuente, A. Merkoçi, Design, preparation, and evaluation of a fixed-orientation antibody/gold-nanoparticle conjugate as an immunosensing label, ACS Appl. Mater. Interfaces 5 (2013) 10753–10759, https://doi.org/10.1021/am4029153.
[224] S. Puertas, P. Batalla, M. Moros, E. Polo, P. del Pino, J.M. Guisán, V. Grazú, J.M. de la Fuente, Taking advantage of unspecific interactions to produce highly active magnetic nanoparticle−antibody conjugates, ACS Nano 5 (2011) 4521–4528, https://doi.org/10.1021/nn200019s.
[225] G. Ruiz, K. Tripathi, S. Okyem, J.D. Driskell, pH impacts the orientation of antibody adsorbed onto gold nanoparticles, Bioconjug. Chem. 30 (2019) 1182–1191, https://doi.org/10.1021/acs.bioconjchem.9b00123.
[226] J.P. Oliveira, A.R. Prado, W.J. Keijok, P.W.P. Antunes, E.R. Yapuchura, M.C.C. Guimarães, Impact of conjugation strategies for targeting of antibodies in gold nanoparticles for ultrasensitive detection of 17β-estradiol, Sci. Rep. 9 (2019) 13859, https://doi.org/10.1038/s41598-019-50424-5.
[227] M. Tonigold, J. Simon, D. Estupiñán, M. Kokkinopoulou, J. Reinholz, U. Kintzel, A. Kaltbeitzel, P. Renz, M.P. Domogalla, K. Steinbrink, I. Lieberwirth, D. Crespy, K. Landfester, V. Mailänder, Pre-adsorption of antibodies enables targeting of

nanocarriers despite a biomolecular corona, Nat. Nanotechnol. (2018) https://doi.org/10.1038/s41565-018-0171-6.
[228] M.C. Lo Giudice, L.M. Herda, E. Polo, K.A. Dawson, In situ characterization of nanoparticle biomolecular interactions in complex biological media by flow cytometry, Nat. Commun. 7 (2016) 13475, https://doi.org/10.1038/ncomms13475.
[229] J. Jeong, W. Kim, L.K. Kim, J. VanHouten, J.J. Wysolmerski, HER2 signaling regulates HER2 localization and membrane retention, PLoS One 12 (2017) https://doi.org/10.1371/journal.pone.0174849.
[230] B. Saha, P. Songe, T.H. Evers, M.W.J. Prins, The influence of covalent immobilization conditions on antibody accessibility on nanoparticles, Analyst 142 (2017) 4247–4256, https://doi.org/10.1039/C7AN01424D.
[231] M.C. Lo Giudice, F. Meder, E. Polo, S.S. Thomas, K. Alnahdi, S. Lara, K.A. Dawson, Constructing bifunctional nanoparticles for dual targeting: improved grafting and surface recognition assessment of multiple ligand nanoparticles, Nanoscale. 8 (2016) 16969–16975, https://doi.org/10.1039/C6NR05478A.
[232] M. Gianneli, E. Polo, H. Lopez, V. Castagnola, T. Aastrup, K.A. Dawson, Label-free in-flow detection of receptor recognition motifs on the biomolecular corona of nanoparticles, Nanoscale. 10 (2018) 5474–5481, https://doi.org/10.1039/C7NR07887K.
[233] Z. Farka, M.J. Mickert, M. Pastucha, Z. Mikušová, P. Skládal, H.H. Gorris, Advances in optical single-molecule detection: on the road to super-sensitive bioaffinity assays, Angew. Chem. Int. Ed. (2019) https://doi.org/10.1002/anie.201913924.
[234] J.Y. Oh, H.S. Kim, L. Palanikumar, E.M. Go, B. Jana, S.A. Park, H.Y. Kim, K. Kim, J.K. Seo, S.K. Kwak, C. Kim, S. Kang, J.-H. Ryu, Cloaking nanoparticles with protein corona shield for targeted drug delivery, Nat. Commun. 9 (2018) https://doi.org/10.1038/s41467-018-06979-4.
[235] L.M. Herda, D.R. Hristov, M.C. Lo Giudice, E. Polo, K.A. Dawson, Mapping of molecular structure of the nanoscale surface in bionanoparticles, J. Am. Chem. Soc. 139 (2017) 111–114, https://doi.org/10.1021/jacs.6b12297.
[236] P. Delcanale, B. Miret-Ontiveros, M. Arista-Romero, S. Pujals, L. Albertazzi, Nanoscale mapping functional sites on nanoparticles by points accumulation for imaging in nanoscale topography (PAINT), ACS Nano (2018) https://doi.org/10.1021/acsnano.7b09063.
[237] S. Lara, F. Alnasser, E. Polo, D. Garry, M.C. Lo Giudice, D.R. Hristov, L. Rocks, A. Salvati, Y. Yan, K.A. Dawson, Identification of receptor binding to the biomolecular corona of nanoparticles, ACS Nano 11 (2017) 1884–1893, https://doi.org/10.1021/acsnano.6b07933.
[238] P.M. Kelly, C. Åberg, E. Polo, A. O'Connell, J. Cookman, J. Fallon, Ž. Krpetić, K.A. Dawson, Mapping protein binding sites on the biomolecular corona of nanoparticles, Nat. Nanotechnol. 10 (2015) 472–479, https://doi.org/10.1038/nnano.2015.47.
[239] F. Wäldchen, J. Schlegel, R. Götz, M. Luciano, M. Schnermann, S. Doose, M. Sauer, Whole-cell imaging of plasma membrane receptors by 3D lattice light-sheet dSTORM, Nat. Commun. 11 (2020) 887, https://doi.org/10.1038/s41467-020-14731-0.
[240] S. Liu, H. Huh, S.-H. Lee, F. Huang, Three-dimensional single-molecule localization microscopy in whole-cell and tissue specimens, Annu. Rev. Biomed. Eng. 22 (2020) https://doi.org/10.1146/annurev-bioeng-060418-052203annurev-bioeng-060418-052203.
[241] F. Xu, D. Ma, K.P. MacPherson, S. Liu, Y. Bu, Y. Wang, Y. Tang, C. Bi, T. Kwok, A.A. Chubykin, P. Yin, S. Calve, G.E. Landreth, F. Huang, Three-dimensional nanoscopy of whole cells and tissues with in situ point spread function retrieval, Nat. Methods 17 (2020) 531–540, https://doi.org/10.1038/s41592-020-0816-x.
[242] T. Ando, S.P. Bhamidimarri, N. Brending, H. Colin-York, L. Collinson, N. De Jonge, P.J. de Pablo, E. Debroye, C. Eggeling, C. Franck, M. Fritzsche, H. Gerritsen, B.N.G. Giepmans, K. Grunewald, J. Hofkens, J.P. Hoogenboom, K.P.F. Janssen, R. Kaufmann, J. Klumperman, N. Kurniawan, J. Kusch, N. Liv, V. Parekh, D.B. Peckys, F. Rehfeldt, D.C. Reutens, M.B.J. Roeffaers, T. Salditt, I.A.T. Schaap, U.S. Schwarz, P. Verkade, M.W. Vogel, R. Wagner, M. Winterhalter, H. Yuan, G. Zifarelli, The 2018 correlative microscopy techniques roadmap, J. Phys. D. Appl. Phys. 51 (2018), 443001. https://doi.org/10.1088/1361-6463/aad055.
[243] D.M. van Elsland, S. Pujals, T. Bakkum, E. Bos, N. Oikonomeas-Koppasis, I. Berlin, J. Neefjes, A.H. Meijer, A.J. Koster, L. Albertazzi, S.I. van Kasteren, Ultrastructural Imaging of salmonella-host interactions using super-resolution correlative light-electron microscopy of bioorthogonal pathogens, ChemBioChem. 19 (2018) 1766–1770, https://doi.org/10.1002/cbic.201800230.
[244] D.P. Hoffman, G. Shtengel, C.S. Xu, K.R. Campbell, M. Freeman, L. Wang, D.E. Milkie, H.A. Pasolli, N. Iyer, J.A. Bogovic, D.R. Stabley, A. Shirinifard, S. Pang, D. Peale, K. Schaefer, W. Pomp, C.-L. Chang, J. Lippincott-Schwartz, T. Kirchhausen, D.J. Solecki, E. Betzig, H.F. Hess, Correlative three-dimensional super-resolution and block-face electron microscopy of whole vitreously frozen cells, Science. 367 (2020) eaaz5357, https://doi.org/10.1126/science.aaz5357.
[245] N.D. Donahue, H. Acar, S. Wilhelm, Concepts of nanoparticle cellular uptake, intracellular trafficking, and kinetics in nanomedicine, Adv. Drug Deliv. Rev. 143 (2019) 68–96, https://doi.org/10.1016/j.addr.2019.04.008.
[246] S. Ashraf, A. Hassan Said, R. Hartmann, M.-A. Assmann, N. Feliu, P. Lenz, W.J. Parak, Quantitative particle uptake by cells as analyzed by different methods, Angew. Chem. Int. Ed. (2019) https://doi.org/10.1002/anie.201906303.
[247] V. Francia, D. Montizaan, A. Salvati, Interactions at the cell membrane and pathways of internalization of nano-sized materials for nanomedicine, Beilstein J. Nanotechnol. 11 (2020) 338–353, https://doi.org/10.3762/bjnano.11.25.
[248] M. Faria, K.F. Noi, Q. Dai, M. Björnmalm, S.T. Johnston, K. Kempe, F. Caruso, E.J. Crampin, Revisiting cell–particle association in vitro: a quantitative method to compare particle performance, J. Control. Release 307 (2019) 355–367, https://doi.org/10.1016/j.jconrel.2019.06.027.
[249] A.J. Chetwynd, K.E. Wheeler, I. Lynch, Best practice in reporting corona studies: Minimum information about Nanomaterial Biocorona Experiments (MINBE), Nano Today 28 (2019), 100758. https://doi.org/10.1016/j.nantod.2019.06.004.
[250] Iver Petersen, Manfred Dietel, Wolf J. Geilenkeuser, et al., EGFR immunohistochemistry as biomarker for antibody-based therapy of squamous NSCLC – Experience from the first ring trial of the German Quality Assurance Initiative for Pathology (QuIP®), Pathology - Research and Practice 213 (12) (2017) 1530–1535, https://doi.org/10.1016/j.prp.2017.09.021.